A new gait parameterization technique by means of cyclogram moments: Application to human slope walking

Ambarish Goswami
INRIA Rhône-Alpes
655 avenue de l'Europe, ZIRST
38330 Montbonnot Saint Martin, France
Ambarish.Goswami@inrialpes.fr

Appeared in
Gait & Posture
August 1998

Abstract

A new parameterization technique for the systematic characterization of human walking gait in diverse external conditions is proposed in this work. By parameterization we mean a quantitative expression of certain gait descriptors as the function of an external parameter, such as the ground slope. The mathematical quantities derived from the geometric features of the hip-knee cyclograms are the main gait descriptors considered in this study. We demonstrate that these descriptors, expressed in a general setting as the geometric moments of the cyclogram contours, can meaningfully reflect the evolution of the gait kinematics on different slopes. We provide a new interpretation of the cyclogram perimeter and discover two potential invariants of slope-walking gait. Experimental slope-walking data obtained at 1° interval within the range of -13° to $+13^{\circ}$ ($\pm 23.1\%$) on a variable-inclination treadmill was used in this study.

The parameterization procedure presented here is general in nature and may be employed without restriction to any closed curve such as the phase diagram, the moment-angle diagram, and the velocity-velocity curves of human gait. The technique may be utilized for the quantitative characterization of normal gait, global comparison of two different gaits, clinical identification of pathological conditions and for the tracking of progress of patients under rehabilitation program.

Keywords: gait parameterization, slope walking, cyclogram, geometric moments, gait kinematics, invariants

1 Introduction

Motivation Characterization of human gait in a quantitative and objective manner has many potential benefits in clinical diagnosis and rehabilitation as well as in the enhancement of our basic understanding of the complicated gait mechanism. In spite of the impressive sophistication of our present day data collection systems, communicable descriptions of certain gait conditions remain surprisingly difficult. Consider describing the progress of a patient's knee joint under rehabilitation care after a knee replacement surgery. A verbal description of the joint's kinematic behavior during a complete gait cycle will be either long or imprecise. What is needed is a comprehensive global picture or an objective capture of information[40] which may be subjected to quantitative analysis.

A second example, which we address in this article, is the evolution of the walking gait in response to a change in the ground slope. In the gait study literature this is known as slope-walking, grade-walking and ramp-walking. Inclined surfaces are frequently encountered in the everyday life but their effect on the gait is relatively under-studied. Ground slope modifies the influence of gravity on the human body, which is known to have a profound effect on the mechanism of locomotion. A visual study of human locomotion, as can be seen in the simplified sketch of Fig. 1, reveals that our gait patterns change considerably, more than is necessary to merely satisfy the kinematic constraints associated with a slope change. Imagine an ideal situation where we have a compact mathematical description which assigns a gait pattern number, say $\mathcal{G}(\alpha)$, for the gait on slope α. As the ground slope changes, this number also changes reflecting the adaptation of the gait. Such a powerful tool would have several practical uses such as the objective characterization of normal gait, global comparison of two different gaits, clinical identification of pathological conditions and the tracking of progress of patients under rehabilitation programs.

Work has already been done in this direction. At the beginning of the last decade [44, 51] used the so-called chain-encoding method[17], a computerized processing technique of line drawings, to correlate the shapes of two cyclograms or two velocity-velocity curves of human locomotion. The geometric congruity of any two shape patterns was consistently reflected by their cross-correlation coefficients. Although the chain-code representation of contours is efficient for computer processing and useful for determining the cross-correlation coefficients, they are, however, abstract numbers and do not give any physical insight into the actual shape of the patterns under study.

Our work is essentially in the same spirit. The objective of this paper is to introduce a general and physically intuitive system of gait representation which may be used qualitatively and quantitatively. Contrary to the simplistic situation portrayed in Fig. 1, in reality, given the complexity of the human gait, we would need several quantities for its complete description. In a multidimensional space such quantities can be represented as a point which characterizes the gait. Different gaits are represented by different points and the evolution of a gait can be characterized by a locus of points in that space.

From a dynamic systems point of view a complete set of "state variables" uniquely describe a system[36]. For example, the joint angle and the joint velocity constitute the state variables of a simple pendulum and can completely represent its motion. Although the level of our current knowledge does not permit us to search for the complete set of state variables of the complex dynamics called the human locomotion, we nevertheless extract some measurable, communicable and meaningful *gait descriptors* to describe locomotion. These gait descriptors may reflect the changes in gait pattern in response to some externally controllable factor or *parameter*. Loosely speaking, a parameter is an imposed condition and a descriptor is the result of the system's response to the imposed condition. Examples of some commonly used gait descriptors are the step length, step frequency, duration of simple and double support phases. A parameter, on the other hand, could be the

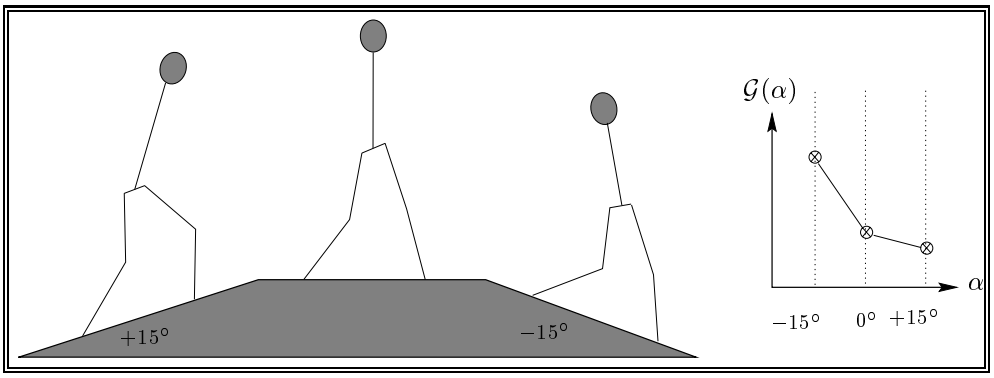

Figure 1: A simplified sketch showing the typical walking patterns on different inclinations and their quantification.

weight of load carried, or as we study here, the ground slope[1].

By parameterization we refer to the systematic and objective description of the evolution of a certain gait descriptor with respect to a parameter. An example of this will be a curve or a mathematical expression relating the load carried and the preferred step length. In the current study, the ground slope has been considered as the only parameter and the gait descriptors are obtained from the geometric features of the cyclograms[20], the rationale behind the choices being given in the following.

Scope of this work The goal of this paper is to introduce a coherent, meaningful, and efficient technique to parameterize the human gait kinematics. The presented method is based upon the geometric moments of the cyclograms of locomotion. As an example of the application of this technique we have considered natural walk on a range of uphill and downhill inclined slopes. We would like to emphasize that the choice of this particular example is motivated by our own research interests (see "Motivation from robotics" below) and the relative familiarity of cyclograms in the biomechanics community and has no special connection with the parameterization method.

In fact, the moment-based parameterization method can be directly applied not only to the cyclograms of other repetitive activities but equally to other representations (such as the phase diagram[30], the moment-angle diagram[18], and the velocity-velocity curves[51]) of repetitive activities.

Why study cyclograms? We postpone the detailed discussion on cyclograms until Section 2. Here we simply point out that although most of the measurable variables of the human gait respond to a parameter change, and parameterization may be performed, in principle, with any of these variables, analysis based on closed trajectories such as cyclograms brings in special advantages. The main reason for this is the fact that the closed trajectories represent forms or shapes that provide us with important insights into the system[8, 23] and are describable by appropriate geometric properties[25, 24]. We will see in the following that as the ground slope gradually changes, the hip-knee cyclogram, obtained by plotting the hip angle versus the knee angle and by omitting the time variables from the two signals, changes its form giving us a clear indication of the modification that the gait is slowly undergoing. Moreover, cyclograms reflect the gait kinematics during the total gait cycle which is different from having other discrete measures such as the step length, or walking speed, which are more common in the literature[35, 53, 52]. A further justification for choosing cyclograms over time-angle plots is the fact that locomotion, a tightly coordinated movement of several limb segments is more naturally grasped as the coupled evolution of two or more joints rather than from the study of individual joint kinematics[8].

Why moment-based shape characterization? One can imagine a number of quantities such as the perimeter and the area, that reflect the geometric properties of cyclogram. Our choice of moment-based characterization of the cyclogram features is justified by the fact that moments (of different orders) can be viewed as a generalization of most of the commonly used geometric features. In the moment-based scheme, the cyclogram perimeter is the zeroth-order moment, the position of its "center of mass" (CM) is a combination of the zeroth-order and the first-order moments. Similarly the higher order moments reflect other features.

Motivation from robotics Before leaving this section we should mention another source of motivation that guided us to this study and which points to the usefulness of cross-domain study. This stems from our challenge of formulating a control law for a biped robot walking on different inclinations [15]. A control law generated for a single slope does not necessarily remain valid for other slopes. Under the assumption that a biological system is efficient or optimal in some sense, we intend to identify "biologically" motivated optimality criteria or at least, to mimic human locomotion with the hope that the robot will be endowed with the same optimal motion. It is possible that the entire dynamics of a complicated system can be generated from a small set of influencing parameters by means of a powerful underlying principle. We have observed that in simplified passive biped robot models the ground slope completely specifies the dynamics[21]. Our long-term objective is to find the principles behind such highly organized motions and to employ them as the control laws.

Structure of this paper The structure of the paper is as follows: Sections 2 and 3 provide the background of this work. Section 2 is devoted to a discussion of cyclograms. It describes the construction and interpretation of cyclograms along with a literature review which we feel is interesting and important. Section 3 consists of a brief review of the literature on slope walking. We also present the experimental protocol for the gait

[1]Some quantities, such as step frequency and walking speed can be either descriptors or parameters (when imposed by a metronome and a treadmill, respectively) depending on the situation. In the literature gait descriptors and parameters are sometime called the dependent variables and the independent variables, respectively.

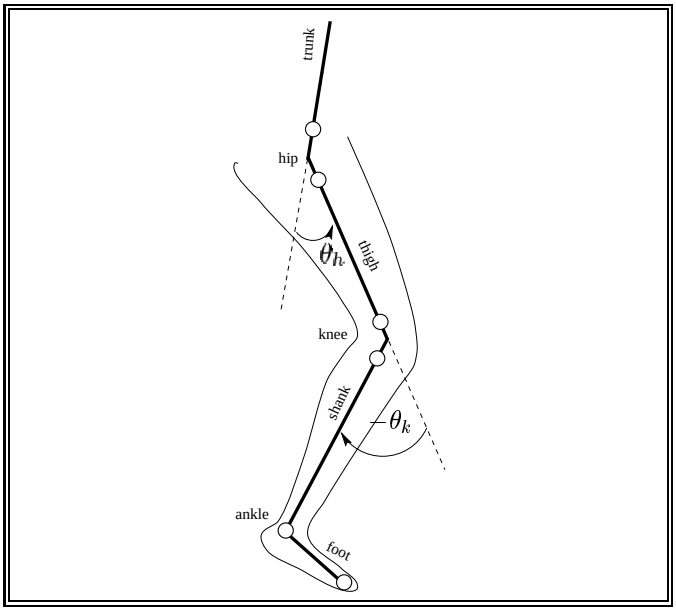

Figure 2: A sketch of the human leg showing the joint angle convention used in this paper. The sketch also shows typical marker positions on the limb segments which are recorded with a camera system.

data used in this work and an overall snapshot of the results (Figs 6 and 3.3). Section 4 forms the core of this paper. First we report the techniques adopted in this paper for the computation of generalized moments of the cyclograms (Section 4.1) and then apply the techniques to calculate various features of the gait cyclograms as they evolve as a function of the ground slope (Section 4.2). Finally Section 5 draws the conclusions and points out some of the open questions.

2 Cyclograms revisited

The concept of cyclograms[2], although known to the biomechanics community, has not been seen very frequently in the literature of the recent past. We review in this section how to construct a cyclogram, how to interpret a typical cyclogram of level walking gait, and provide some highlights of the historical developments of cyclograms.

2.1 What are cyclograms and how to construct one?

Commonly human gait data consist of the recorded positions of retro-reflective markers taped on the skin at the extremities of the limb segments (the thigh, the shank etc.) of a subject. The angles between each two segments are subsequently calculated assuming the segments to be idealized rigid bodies. Fig. 2 shows a sketch of the right leg of a subject and indicates the joint angle assignment used in this paper. θ_h and θ_k are the hip angle and the knee angle, respectively.

Fig. 3(a) and 3(b) show two time-angle plots corresponding to the knee and the hip angle during one gait cycle. A cyclogram is formed by ignoring the time axis of each curve and directly plotting knee angle VS hip angle as shown in Fig. 3(c). A formal way of describing cyclograms is to identify them as the so-called "parametric curves". A parametric curve is obtained by directly plotting the associated variables, $x_1(\lambda), x_2(\lambda), \ldots, x_n(\lambda)$, where each variable is a function of a parameter, λ. In the present context the joint angles are the variables and time is the parameter. One advantage of this formal definition is that it can be extended to include other curves such as the phase diagrams[4, 31, 30] and the moment angle diagrams[18].

Please note that for the joint angle assignment convention adopted in this paper, the planar cyclograms have a counter-clockwise direction. Note also that although the points on the curves 3(a) and 3(b) are equally spaced this is not so for the points on the cyclogram. The spacing of points on a cyclogram is directly proportional to the respective joint velocities. When the joints move slowly, the points are close spaced.

[2] A web search for the keyword "cyclogram" points to numerous articles on cyclograms related to the functioning of instruments used in space flights!

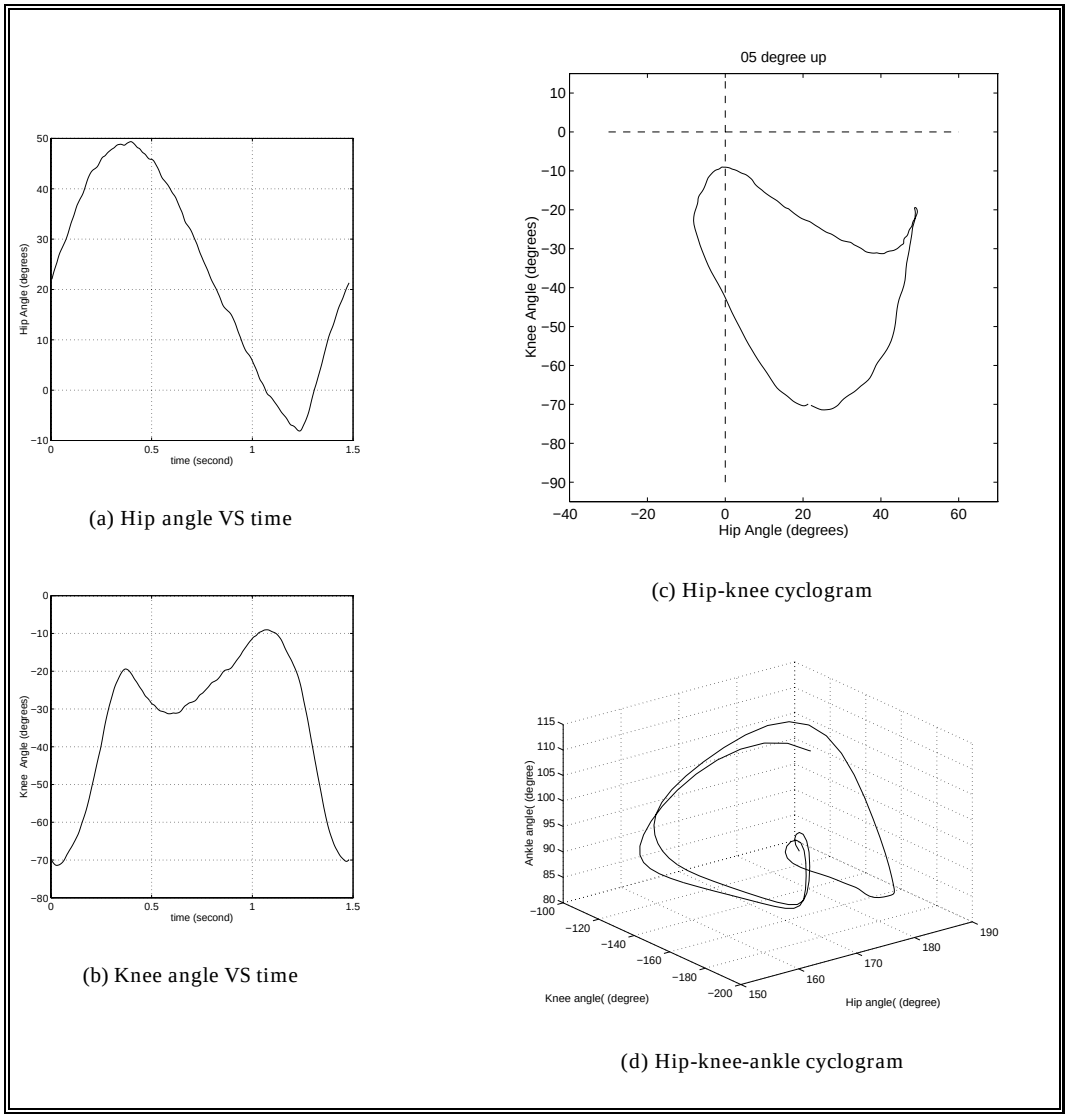

Figure 3: Construction of a hip-knee cyclogram from individual hip and knee joint data for a 5° uphill walk. The counter-clockwise direction in the cyclogram corresponds to the forward progression of gait. Data for Fig.(d) was provided by the Gait Lab, University of Waterloo, with permission of Prof. D.A.Winter.

Steady human locomotion is almost periodic and cyclograms obtained from joint angle signals of equal time lengths, such as Figs. 3(a) and 3(b), will be an approximate cycle. The cyclogram features that we use in this paper for parameterization are essentially valid for such contours but for algorithmic simplicity we will assume that the contours are closed.

Finally, cyclograms do not have to be planar although for visualization purposes we should limit ourselves to the 3 dimensional space. Fig. 3(d) shows a 3-dimensional cyclogram obtained by simultaneously plotting the hip, the knee and the ankle joint trajectories. See [55] for examples of some traditional 3-d hip-knee-ankle cyclograms and [6] for 3-d cyclograms obtained from absolute elevation angles of thigh-shank-foot.

Cyclograms and phase diagrams We have mentioned earlier that our parameterization method is equally applicable to other cyclic representations of locomotion such as the phase diagram[4, 30, 31], the moment-angle diagram[18], and the velocity-velocity curves[51]. Since the phase diagram has a formidable following and are physically more fundamental than the cyclograms, it is important to distinguish between the two.

The phase diagram of a dynamic system resides in its phase space. The two most popular definitions of the phase space describe it as the space consisting of the generalized coordinate / generalized momentum variables and the generalized coordinate / generalized velocity variables[3, 26]. The second definition, according to which the phase space is identical to the state space, is used in the biomechanics community. A state of a

system is represented by a point in its phase space and the evolution of the system is given by a trajectory in the phase space, called the phase diagram.

In our current context, phase space would contain the joint displacements *and* the joint trajectories of the movement under study and therefore can be considered as a superset of cyclograms, which contain the joint displacements only. However, since neither the entire phase diagram nor the entire cyclogram of a multi-degree of freedom system is graphically visualizable, we have to be content with lower-dimensional (most frequently 2-dimensional) projections of these diagrams. These planar versions of the diagrams carry significantly different information. A planar angle-angle cyclogram provides information about the posture of the leg and the coordination of two joints but is silent about the velocities involved. A planar angle-velocity phase diagram, on the other hand, represents the complete dynamics of a single joint but provides no information about the coordination of two joints.

Both cyclograms and phase diagrams are important signatures of locomotion and each has its own merits. Although traditionally cyclograms have received more exposure in the biomechanics community, phase diagrams have started to be noticed as well[29, 30, 31].

2.2 Interpretation of a typical cyclogram

It is instructive to study a typical cyclogram and relate its important features with the characteristics of the normal gait. We refer to Fig. 2.2 (and Fig. 2 for the joint angle assignment convention) in this section. The complete gait cycle is divided into 10 equal temporal segments and are marked by '*' on the cyclogram. Certain important events in a gait cycle are marked with an 'o' on the cyclogram along with a corresponding short description.

Let us travel along the cyclogram from the instant of heel-strike (marked hs in the figure). The period just after the heel-strike is represented by an almost vertical line characterizing the rapid knee flexion and little hip movement. The shock created by the heel impact with the ground is quickly attenuated during this period. After foot-flat (ff) the hip begins to extend along with the knee shown by the inclined line connecting foot-flat and mid-support (msu). The time period between hs and (c)to is called the loading phase which occupies about $10 - 12\%$ of the gait cycle. The next phase, the weight-bearing phase, is characterized by an extending knee.

The effect of propulsion can be seen in the cyclogram at the end of the stance phase. The hyper-extension of the hip reaches a maximum and gradually reverses, and the previously extending knee smoothly translates to flexion which continues steadily through stance into swing phase. The toe-off occurs before the knee is fully flexed.

Typically the swing phase starts at 0° thigh extension angle and a knee flexion of about 80% of the maximum. By mid-swing the flexion of the thigh is complete and the knee, after reaching its maximum flexion is extending in preparation for the next foot placement. There is almost no thigh movement between the mid-swing and the heel-strike and the phase is effected by a steady reduction of the knee flexion.

We conclude this section by presenting some of the highlights of the historical development of the concept of cyclogram.

2.3 History of cyclograms

A literature search of the cyclogram reveals the name of Grieve as the first to propose the use of cyclograms (they were called the angle-angle diagrams) [22, 23]. Grieve argued that a cyclic process such as walking is better understood if studied with a cyclic plot such as a cyclogram and proposed the inclusion of auxiliary information such as the time instants of heel-strike and toe-off in the cyclogram to render them more informative. Observing the deviations of gait characteristics on cyclograms he suggested that the deviations in the gait characteristics cannot be adequately modeled as a mean square deviation since the deviations are not random and that both the direction and the magnitude of deviations in combination with others have to be considered and that only certain combinations of deviations are to be regarded as "normal". Grieve also recognized on the cyclogram the prominent shock absorption phase during heel-strike and the "whiplash effect" of the leg at faster gaits.

Six different cyclograms corresponding to six different walking speeds for each of hip-knee, hip-ankle, and knee-ankle combinations were presented in [37].

Cyclograms from standing broad jump, stair climbing, race walking as well as normal walking at different speeds are presented in [8]. One important contribution of this paper is the demonstration that cyclograms, in synergy with other kinematic representations of multi-joint movements, can become a powerful analytical tool.

We encounter the subsequent work of Milner and his colleagues during the seventies up until 1980 [40, 25, 24]. Use of cyclograms as a means of tracking the progress of patients undergoing total hip joint recon-

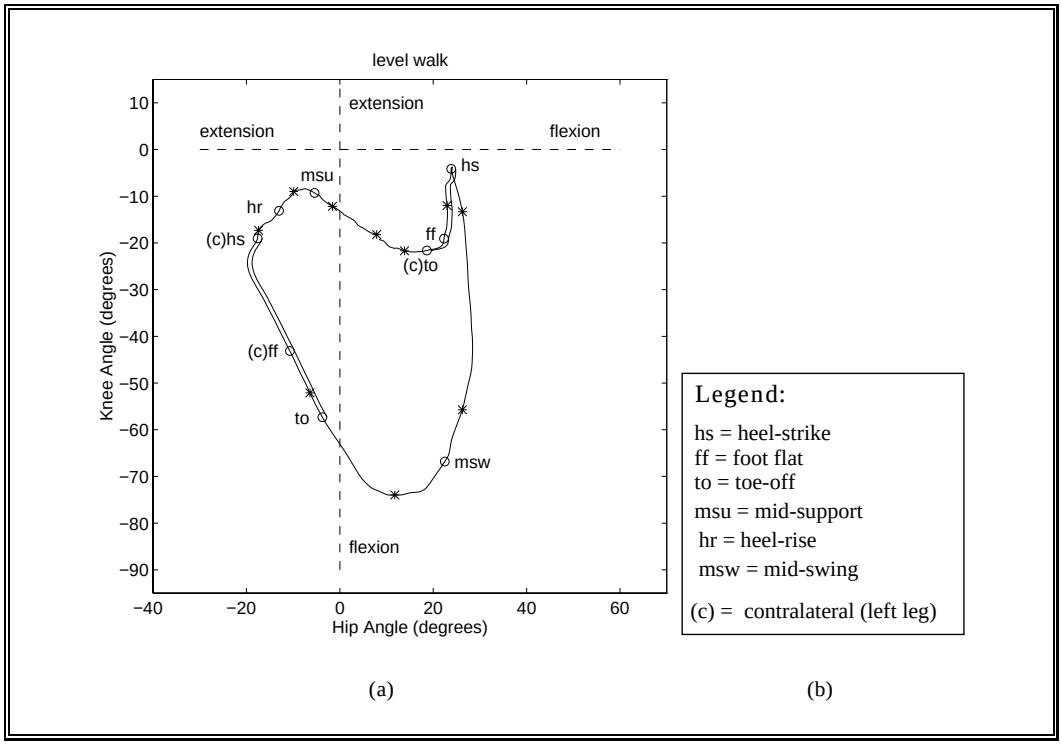

Figure 4: A typical hip-knee cyclogram for level walk (adapted from [9]). See Section 2.2 for description.

struction was explored in [40]. It was demonstrated that, as one might expect, the cyclograms of abnormal gaits are geometrically very different and are easy to visually identify from those obtained for normal gaits. The same work also reported the evolution of the geometric form of the cyclogram as a function of walking speed[3]. So far, no attempt has been made to analytically study the quantitative geometric characteristics of the cyclograms. This was addressed in [25, 24] and subsequent papers.

The importance of a quantitative study of cyclogram shapes in order to extract relevant numbers, to be used as gait descriptors concerns [25]. Only normal healthy gaits at different speeds were considered in this article. Three geometric characteristics of the closed-loop cyclograms, the perimeter P, the area A, and the dimensionless ratio $\frac{P}{\sqrt{A}}$ were considered. It was shown that although the perimeter and the area of cyclograms are approximately linearly related to the average walking speed, the quantity $\frac{P}{\sqrt{A}}$ stays roughly constant. This latter quantity can thus be called an *invariant* of walk as far the speed is concerned. Cyclogram area is intuitively related to the conjoint range of the angular movements concerned. The larger the range, the larger the cyclogram area. In a second concurrent paper [24] the same authors studied cyclograms obtained from above-knee amputee gait and cerebral palsy gait. The quantity $\frac{P}{\sqrt{A}}$ again reflected the abnormalities in these gaits.

[10] compares the gait patterns of human and dogs by means of cyclograms (called cyclographs and angle / angle diagrams in the paper). It emphasized the utility of cyclic traces of joint variables by pointing out that a coordinated motion of a leg is to be perceived as an interaction between two or more limbs rather than a phenomenon of isolated joint movements over time. The cyclogram pattern is noted to be an extremely stable mechanism to identify gait behavior.

The geometric similarity of two cyclograms or two velocity-velocity curves of locomotion was computed[44, 51] by employing the discrete chain-encoding representation[17] of the curves. Our work follows the same philosophy, that of the quantification of the similarity of different movement patterns, which is nicely articulated in[51].

In [9] the evolution of cyclograms as a function of the walking speed is considered. Three different levels of speed corresponding to 0.5 st / s (slow), 0.9 st / s (medium), and 1.3 st / s (fast) were considered[4]. The cyclograms are annotated with additional information such as the important events. In Fig. 2.2 we have followed the same trait. Two pathological cases were considered to show how a "standard" cyclogram and superimposed

[3]Five different speeds, from 2.34 km / h to 6.91 km / h were studied.
[4]Stature / second. Speed is normalized by the leg length.

standard deviation data can be used to detect abnormal gait conditions.

In an unpublished (and personally communicated) article [49] level and uphill and downhill slopes of 10%, 20% were considered. It was found that walking speed at all grades was slightly reduced compared to level walking. The hip-knee cyclograms used in this article demonstrated that downhill walk is associated with larger knee flexion in stance phase and reduced hip flexion during swing phase. In uphill walking both the knee and the hip are flexed at foot contact and in the swing phase.

Neural network has been used to perform automated diagnosis of gait patterns represented by cyclograms[2]. Once trained, the network can identify with a 83.3% success rate the three different conditions – normal gait, a gait with unequal leg length and a gait with unequal leg weight. The view that kinematic analysis is of great help in the diagnosis and rehabilitation of locomotor disorders such as cerebral palsy and spastic diplegia is reinforced[2].

3-d cyclograms have been recently used in a different context, in order to show the modal bifurcation displayed in human locomotion[55]. Traditionally, cyclograms are drawn with the inter-segmental joint variables. A remarkable recent result shows that if instead, the cyclograms are constructed from the absolute elevation angles of the limbs (angles made by thigh, shank and foot with the vertical), the resulting 3-d cyclogram of human locomotion lies on a plane! This means that a strong underlying strategy is in action during locomotion.

Although it is about running gait (not walking) gait, [7] reports one the most systematic analyses on the effect of inclined surfaces performed with cyclograms. Here cyclograms were used to demonstrate the gradual change in the running gait as a function of the slope and the speed of running. The increased range of the cushioning phase knee flexion was noted as a remarkable feature for downhill running as we also observe in our cyclograms for downhill walking.

The value of objective description of human locomotion can be appreciated from the recent work[30, 31] on the phase diagram. In [30] the periodicity of gait was determined from the Poincaré map[3] of the locomotion whereas in [31] the difference in the area inside the phase diagrams obtained from the left and the right leg of the same person was successfully utilized to quantify the gait asymmetry in post-polio patients.

Before getting into the shape analysis of cyclograms we will briefly study the problem of slope walking in the next section.

3 Slope walking

3.1 Brief literature review

In order to facilitate the interpretation and evaluation of our results we briefly review the existing literature on slope walking. The review is not meant to be exhaustive and only the results that are comparable to ours are mentioned.

One of the first papers in this area, [14] reported that the ground slope within the range of 0 to 10% did not have any significant influence on the stride length and the step rate.

[50] in a study of level walk and walk on slopes of $\pm 10\%$ $\pm 20\%$ noticed that average chosen walking speed decreases both for uphill and downhill slopes. Increased knee and hip flexion of the forward limb during contact was considered to be the major influence of uphill walk whereas those for downhill walk were an increased knee flexion of the supporting limb during contact and decreased thigh flexion in late swing.

In [53] gait data from 5 healthy male subjects walking on the level as well as on $+5\%$ and $+10\%$ slopes. The authors found that the on an uphill slope the subjects took shorter steps at slow speeds and longer steps at fast speeds compared to those in the level walk.

Level walk and walk on uphill and downhill slopes of 3°, 6°, 9° and 12° were considered in [35]. The authors' found that for higher slopes (both uphill and downhill) the walking speed significantly decreased. Whereas on uphill slopes the speed reduction was caused by a reduction in the cadence, on downhill slopes it was caused by a reduction in the step length. The findings point towards the asymmetry in the way human beings respond to uphill and downhill slopes.

In the study reported in [45] only downhill slopes of -4%, -8%, -12%, -16% [5] along with the level walk were considered. It was reported that the influence of ground slope on the temporal parameters of gait was not statistically significant. The authors observed two main gait adaptation strategies in downhill slopes. In the first strategy, perhaps unexpectedly, the subjects lean forward and increase the step length and in the second the subjects stay relatively erect but decrease the step length.

[47] studied the gait of urban pedestrians on uphill and downhill slopes up to 9°. A detailed analysis shows that for uphill walking the mean walking speed, cadence (steps / min), and step length decreases significantly with increasing slope. For downhill walk, the speed and cadence did not significantly vary with slope but the

[5] an $x\%$ slope corresponds to an angle of $(tan^{-1}(\frac{x}{100}))^\circ$.

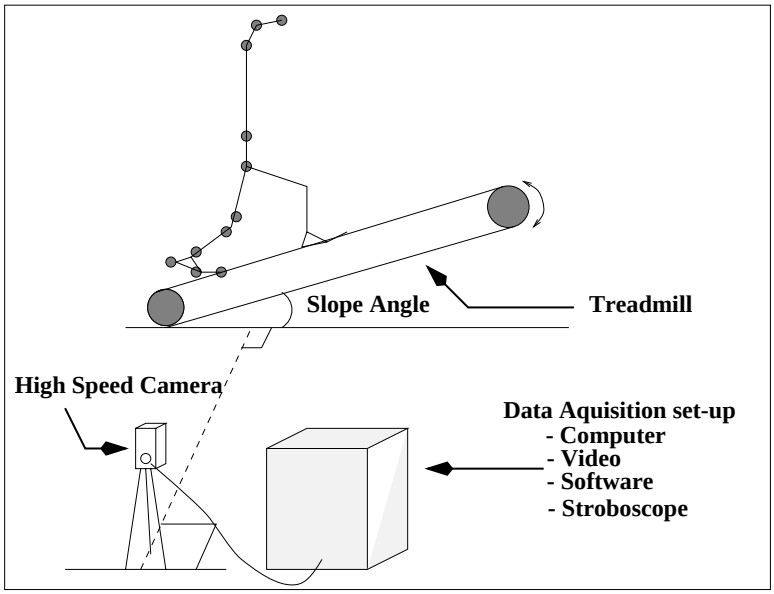

Figure 5: The experimental set-up.

step length significantly decreased with increasing slope. It is mentioned here that [16] found no significant differences between the uphill and downhill gaits of urban pedestrians on up to 4° slope.

[42] studied the influence of downhill slopes on the mechanism of fall, which is a serious issue especially for the elderly. The authors also considered the friction requirements of the shoe for different inclinations. The energy considerations of slope-walking were considered in [46, 5].

3.2 Experimental method

The data presented in the paper are obtained from two healthy male subjects (28 and 23 years of age, 181cm and 182cm height, respectively) without any history of lower extremity injury. 11 flat retro-reflective markers of 1-2 cm diameter were taped onto the skin at the anatomical landmarks of the subjects. The marker on the shank were placed at the tibial epicondyle and the external malleolus, and those on the thigh were at the greater trochanter and the lateral femoral condyle. The knee angle is defined as the angle between the straight lines joining the two shank markers and the two thigh markers. The hip angle, on the other hand, is the angle between the line joining the two thigh markers and the line joining the marker at the greater trochanter and another at the iliac crest[6]. A motor-driven variable inclination treadmill from TechMachine was used for all the trials. The subjects chose the "most comfortable" treadmill speed for each slope. A NAC HSV400 video camera registered the marker positions. The camera axis was perpendicular to the length of the treadmill thus permitting us to register the sagittal plane motion of the subjects. The registered data were processed taking into account the treadmill speed. The marker position data was filtered with a 4^{th}-order Butterworth filter with a cut-off frequency of 12 Hz. See Fig. 5 for a sketch of the experimental set-up.

The inclination of the treadmill was varied from -13° to $+13^\circ$ with data collected at each 1° interval. To simplify the logistics, two separate sessions, one each for uphill walk and downhill walk, were organized. However, in order to minimize the possibility of anticipation on the part of the subjects, the sequence in which the slopes were changed was unknown to the subjects. The subjects wore soft shoes.

This paper uses data from only one of the subjects. Out of a complete 8 minutes of walk on each slope, we have selected one cycle which is representative of the particular slope and which does not show any transients. Other than filtering the time-angle data as mentioned earlier, we do not adopt any sophisticated segmentation technique (such as [12]) to extract perfect cycles. Despite this, the trend in the evolution of the gait descriptors as a function of the ground slope is clearly identifiable which illustrates the efficiency and robustness of the proposed method. However an explanation is called for as the common practice is to average the gait data over several different individuals and / or several trails from the same individual.

Averaging generally improves the robustness of the data by reducing the effects of the statistical outliers. An unavoidable consequence is the suppression of the characteristics features of the individual gaits. It is

[6]We realize that the definition of "joint angle" under this convention is less than satisfactory. Systematic definition of joint angles from human gait data is a topic of our ongoing study.

indicated in the literature that gait adaptation strategies in a changed environment often vary from person to person[45] and by doing a gross averaging we may risk losing some of these subtle strategies adopted by individuals. We align ourselves with the view[41] that it is important to study the responses of individual subjects.

Thus, although the data used here is a representative of the normal gait, we do not imply that the specific gait descriptor values extracted from the data will perfectly match those obtained from other individuals. The important point is that the parameterization technique is equally valid for the averaged data as well as for the data from an individual subject.

3.3 A snapshot of the result

In Fig. 6 and Fig. 3.3 we show the gradual evolution of cyclograms on inclined slopes. Fig. 6 shows cyclograms on downhill slopes changing from 0° to -13° and Fig. 3.3 shows cyclograms on uphill slopes changing from 0° to $+13^\circ$. Data obtained for each 1° change in the ground slope provides us with a rich database appropriate for the parameterization techniques.

Some of the interesting qualitative features of slope-walking are visibly discernible from Figs. 6 and 3.3. Fig 6 shows the prominent impact cushioning phase for downhill slopes marked by a virtual reversal of the cyclogram trajectory. This is to be compared with the cyclograms for uphill slopes to note the utter lack of impact in the latter.

The range of hip movement steadily diminishes for downhill slopes as is evident from the horizontally "squashed" form of the cyclogram at these slopes. The range of hip movement has, in fact, a linearly increasing trend as we go from -13° to $+13^\circ$ slope, see plot Figs. 8(b) and 8(c). The knee angle behaves in an opposite, but remarkably symmetric manner. The total range of knee angle is a linearly decreasing function of slope (as we go from -13° to $+13^\circ$) as shown in Figs. 8(a) and 8(d). Here we note the symmetric nature of the Fig. 8(a) and 8(b). Quantitatively we can say that the range of knee joint (hip joint) decreases (increases) at the rate of 1.5° per degree increase in the ground slope.

Fig. 9 presents the evolution of the knee and hip angles at heel-strike (considered to be located at the point of "folding" of the cyclogram) along with their quadratic fits. Again it is interesting to note the remarkably symmetric nature of evolution of the hip and the knee angles[13].

4 Moment-based features of cyclograms

The identification and classification of plane closed curves, a subject of study often called 2D shape recognition, is a topic of considerable research interest in the fields of Computer Vision and Pattern Recognition. The objective of the research, simply stated, is to identify, classify, and describe 2D objects or scenes with unknown position and orientation, usually from their noisy images. Thus in the Pattern recognition applications, there is a need for selecting certain geometric properties of the object which are as insensitive as possible to the variations in size, displacement, orientation and the presence of noise. These properties are called the *shape descriptors* of the object. The field of computerized (handwritten) character recognition also has similar requirements.

There are several techniques for quantifying planar shapes and the reader is directed to[33, 32, 19] for information on the traditional methods. Here we concentrate on the use of moments for shape identification and classification. The first significant work on the use of moments in identifying 2D shapes is by [28]. The usefulness of this technique stimulated a lot of research and algorithms were developed to refine and extend the method and make it robust against noise[48]. Some relatively recent articles in this domain are [39, 1]. Efficient algorithms to compute moments were presented in [34, 38, 54]. In this paper we have adapted the method in [34] to compute perimeter-based moments.

It can be shown that the infinite set of moments uniquely determine a planar shape and vice-versa[33]. In other words, the moments are the axes in an infinite-dimensional space in which a contour is represented by a unique point. It should be added that the higher-order moments are sensitive to noise and harder to interpret physically.

Area-based moments VS perimeter-based moments Let us recognize certain distinctive characteristics of the closed contours whose geometric features we study and attempt to quantify here. These characteristics will help us choose the proper shape computation technique. First of all, as shown in the inset of Fig. 10, the cyclograms are not continuous curves but are polyline contours or simply irregular polygons. Second, the contour is rather unsmooth which is often a function of the amount of noise in the overall data registration system. Third, the plane cyclograms frequently consist of self intersecting loops.

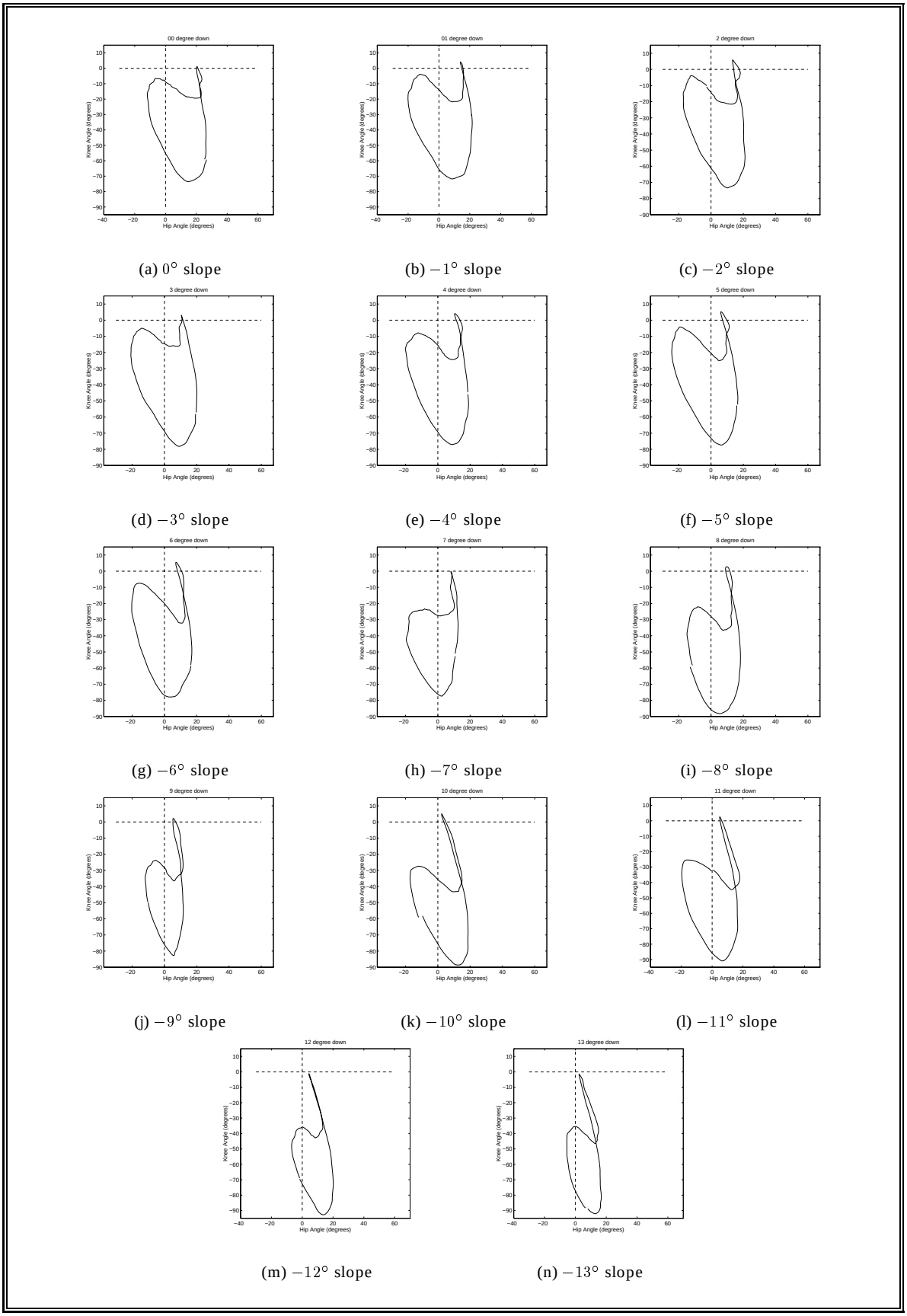

(a) 0° slope (b) -1° slope (c) -2° slope

(d) -3° slope (e) -4° slope (f) -5° slope

(g) -6° slope (h) -7° slope (i) -8° slope

(j) -9° slope (k) -10° slope (l) -11° slope

(m) -12° slope (n) -13° slope

Figure 6: Hip-knee cyclograms for walking downhill. Each diagram is to be followed in the counter-clockwise direction. Refer to Fig. 2.2.

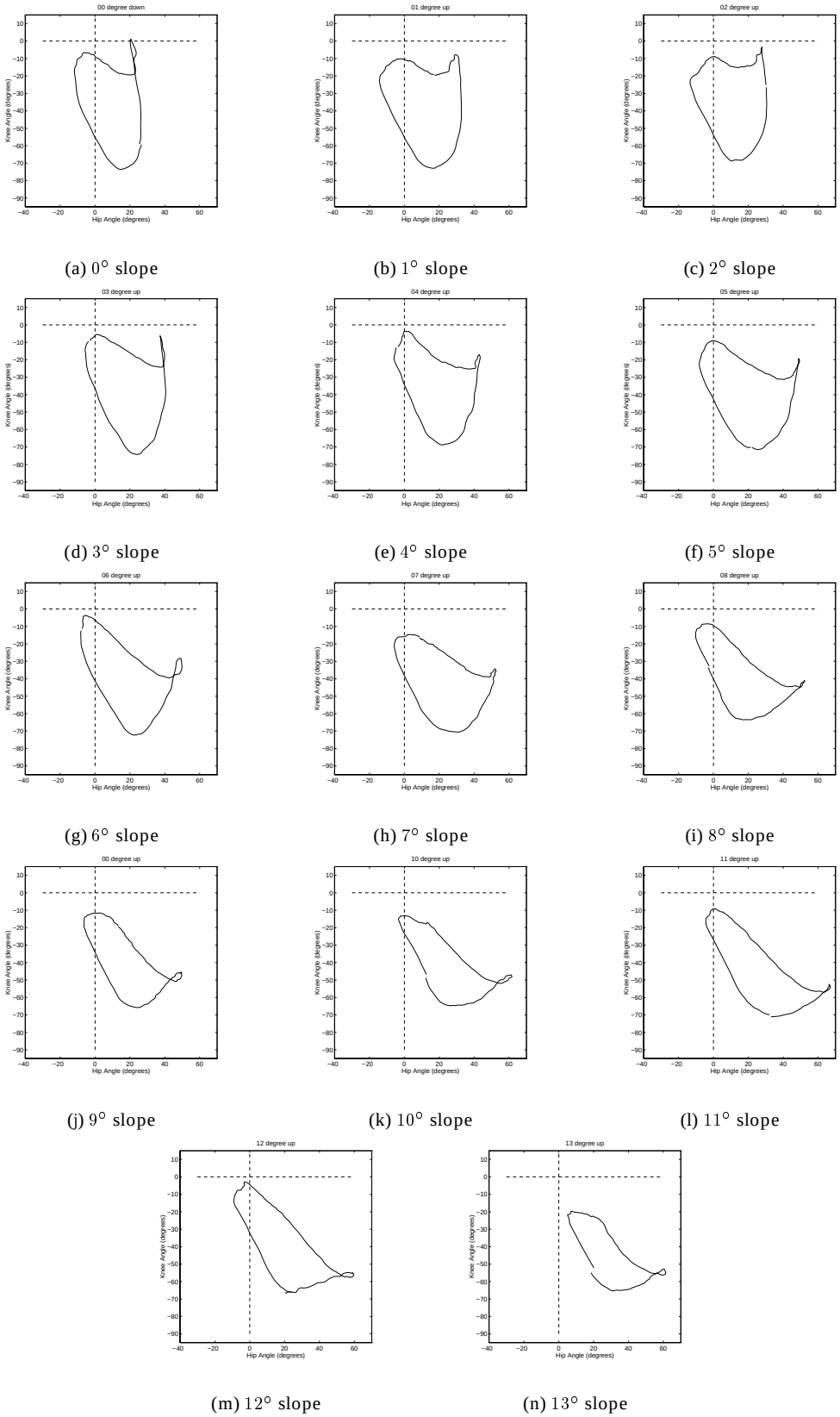

(a) 0° slope (b) 1° slope (c) 2° slope

(d) 3° slope (e) 4° slope (f) 5° slope

(g) 6° slope (h) 7° slope (i) 8° slope

(j) 9° slope (k) 10° slope (l) 11° slope

(m) 12° slope (n) 13° slope

Figure 7: Hip-knee cyclograms for walking uphill. Each diagram is to be followed in the counter-clockwise direction. Refer to Fig. 2.2.

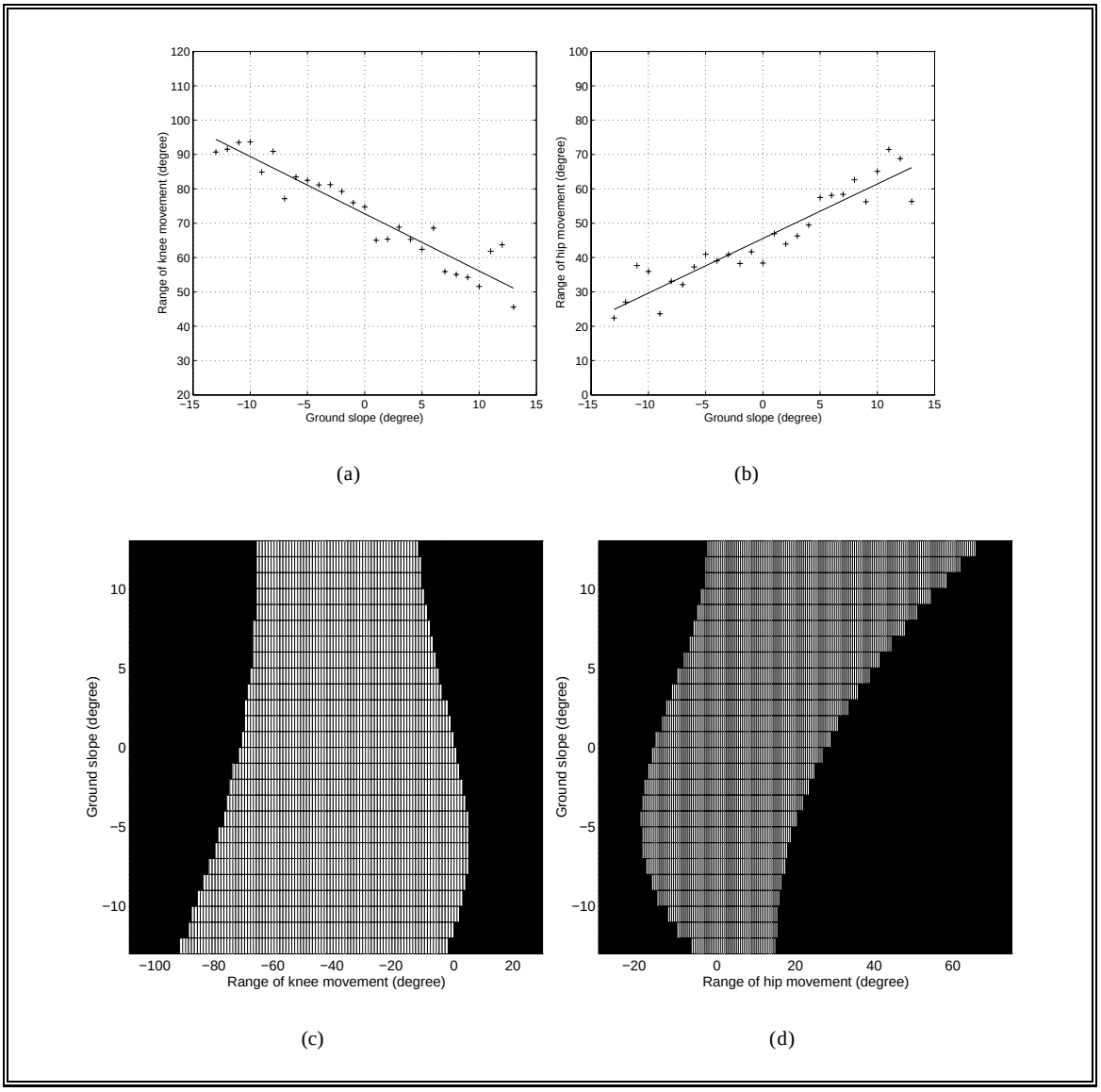

Figure 8: Evolution of the total range of movement of a) knee and b) hip angles with change in ground slope. Both the curves are shown with straight lines of least-squares fit, c) and d) represent the actual joint ranges of the knee and hip, respectively as functions of slope.

Traditionally, the Pattern Recognition community has utilized the *area-based* moments of binary 2D shapes. Whereas we could use the same techniques here, we prefer the *perimeter-based* moments of cyclogram contours for three main reasons. First, the cyclogram is not the boundary of any real object but is *the* object whose shape characterization is our goal. Second, the perimeter-based moments are equally applicable to higher dimensional cyclograms (θ_{hip} VS θ_{knee} VS θ_{ankle}), see Fig. 3(d), where the area-based moments lose their meaning. Third, the 2D cyclograms often consist of self-intersecting loops and these are free to lie partially or entirely inside another loop. There are situations where the interpretation of what area inside a curve might mean is complicated. Although we do not treat the cases of self-intersecting at present they do occur frequently in the form of self-intersecting multiple loop 2D cyclograms. The interpretation of area is especially complicated for a self-intersecting cycle that lies partially or entirely inside another loop. On the other hand, perimeter-based moments are not very reliable for extremely noisy data. The general effect of noise in the data is the roughness of the trajectory. This may significantly increase the perimeter of the cyclogram without affecting its area. This intuitive idea is explored more analytically in [43].

In order to calculate the perimeter-based moments we make a physical analogy of the cyclogram with a thin polygonal wire loop with uniform mass distribution along its length. We find the exact moment of each side of the n-gon by an integral and sum these to obtain the overall moment of the contour. The procedure is

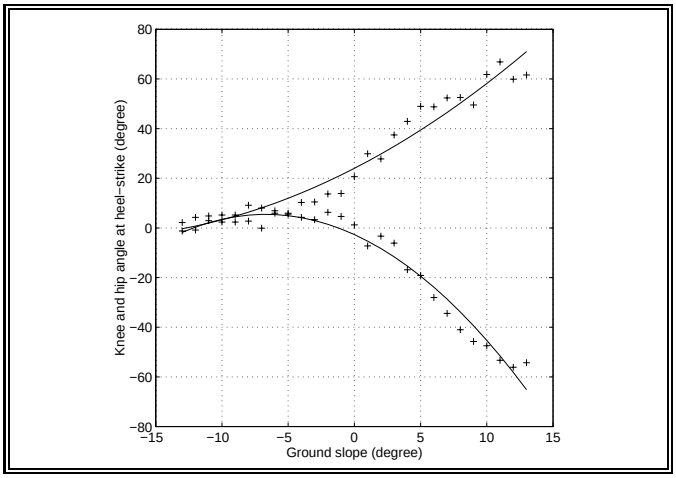

Figure 9: Evolution of the knee and hip angle at heel-strike along with their quadratic fits.

analogous to that of calculating area-based moments but the numerical values obtained are obviously different.

4.1 Computation of generalized moments

In this section we formally introduce the idea of generalized moments, show their relationships to several basic features of the contour and present a simple recursive formula (following [34]) to calculate the generalized moments of higher orders.

The two-dimensional moments of order $(p+q)$ of a curve of length Lin the $x-y$ plane are,

$$M_{pq} = \int_0^L x^p y^q dl. \tag{1}$$

In the cyclogram plane $x = \theta_h$ and $y = \theta_k$. The starting point on the curve, corresponding to $L = 0$ does not have any influence on the moment values. The choice of origin $\theta_h = 0$, $\theta_k = 0$ does not have a significant effect but is fixed by our angle convention.

The above equation can be modified for a contour comprising n straight line segments as follows,

$$M_{pq} = \sum_{i=1}^{n} \int_0^{L_i} x^p y^q dl = \sum_{i=1}^{n} \mu^i(p,q), \tag{2}$$

where L_i is the length of the i^{th} segment and $\mu^i(p,q)$ is expressed as

$$\mu^i(p,q) = \int_0^{L_i} x^p y^q dl = \int_{min(x_i,x_{i+1})}^{max(x_i,x_{i+1})} x^p y^q \sqrt{(1+s_i^2)} dx. \tag{3}$$

In the above equation the infinitesimal line segment dl has been replaced, via a change of variables, by $\sqrt{(1+s_i^2)}dx$, where s_i is the slope of the i^{th} line segment, a constant. Also we need to make sure that the integration is always performed from the minimum to the maximum of the two numbers x_i and x_{i+1}. With this implied order we will henceforth simply put the integration from x_i to x_{i+1}.

The constant $\sqrt{(1+s_i^2)} = t_i$ can be taken outside the integral. The variable y for the i^{th} line segment can be expressed as

$$y = s_i x + (y_i - s_i x_i) = s_i x + u_i, \tag{4}$$

u_i being another constant. With these modifications, $\mu^i(p,q)$ is rewritten as

$$\mu^i(p,q) = t_i \int_{x_i}^{x_{i+1}} x^p (s_i x + u_i)^q dx. \tag{5}$$

Following the procedure presented in [34] for the area-moments of a 2D shape, we search for recursive equations to compute the higher-order perimeter-based moments. To that goal we do the following

$$\mu^i(p,q) = t_i \int_{x_i}^{x_{i+1}} x^p (s_i x + u_i)^{q-1}(s_i x + u_i) dx. \quad (6)$$

$$= t_i [s_i \int_{x_i}^{x_{i+1}} x^{p+1}(s_i x + u_i)^{q-1} dx + u_i \int_{x_i}^{x_{i+1}} x^p (s_i x + u_i)^{q-1} dx]. \quad (7)$$

The recursive equations are of the form

$$\mu^i(p,q) = s_i \mu^i(p+1, q-1) + u_i \mu^i(p, q-1). \quad (8)$$

Any moment of the form $\mu^i(p,0)$ such as $\mu^i(0,0)$, with which the recursion must begin, can be calculated by a simple integration

$$\mu^i(p,0) = t_i \int_{x_i}^{x_{i+1}} x^p dx = \frac{x_{i+1}^{p+1} - x_i^{p+1}}{p+1}, \quad (9)$$

.

We have to take into account the situation where the considered line segment is vertical; the slope of this line is not defined. In this case, instead of re-parameterizing dl with the variable x we rather do it with y, as $dl = \sqrt{(1 + \frac{dx}{dy})} dy$. The quantity $\frac{dx}{dy}$, the inverse of the slope, is equal to zero for a vertical line segment. The expression for the generalized moments for a vertical line segment therefore reduces to,

$$\mu^i(p,q) = \int_{y_i}^{y_{i+1}} x_i^p y^q dy = \frac{x_i^p (y_{i+1}^{q+1} - y_i^{q+1})}{q+1}. \quad (10)$$

The first few moments of a straight line segment are presented in the Table 1.

Table 1: Moment computation of line segments

moment	non-vertical segments	vertical segments
$\mu^i(0,0)$	$t_i(x_{i+1} - x_i)$	$y_{i+1} - y_i$
$\mu^i(1,0)$	$t_i \frac{(x_{i+1}^2 - x_i^2)}{2}$	$x_i(y_{i+1} - y_i)$
$\mu^i(0,1)$	$s_i \mu^i(1,0) + u_i \mu^i(0,0)$	$\frac{y_{i+1}^2 - y_i^2}{2}$
$\mu^i(2,0)$	$t_i \frac{(x_{i+1}^3 - x_i^3)}{3}$	$x_i^2(y_{i+1} - y_i)$
$\mu^i(1,1)$	$s_i \mu^i(2,0) + u_i \mu^i(1,0)$	$\frac{x_i(y_{i+1}^2 - y_i^2)}{2}$
$\mu^i(0,2)$	$s_i \mu^i(1,1) + u_i \mu^i(0,1)$	$\frac{y_{i+1}^3 - y_i^3}{3}$

The recursion process must follow the sequence:

$$\begin{array}{lllll} \mu^i(0,0) & & & & \\ \mu^i(1,0) & \mu^i(0,1) & & & \\ \mu^i(2,0) & \mu^i(1,1) & \mu^i(0,2) & & \\ \mu^i(3,0) & \mu^i(2,1) & \mu^i(1,2) & \mu^i(0,3) & \\ \mu^i(4,0) & \mu^i(3,1) & \mu^i(2,2) & \mu^i(1,3) & \mu^i(0,4) \end{array}$$

4.2 Parameterization of cyclogram features

We now consider the parameterization of the moment-based descriptors of the cyclograms as they evolve as the ground slope changes from -13° to $+13^\circ$. For each case, we define the gait descriptor, plot its evolution as a function of the ground slope and discuss its trend.

4.2.1 Perimeter

The perimeter of a cyclogram is simply its zeroth moment M_{00}. In Fig. 11(a) we present the evolution of the cyclogram perimeter normalized against the perimeter at 0° slope (which is equal to 212.88°). The perimeter is a linearly decreasing function of the ground slope as can be inferred from the straight line in the figure representing the least-squares error line. Although the "jerkiness" of the joint motion was given as a possible reason of an increase in the perimeter of similar curves in [25], it is unlikely to be reason here.

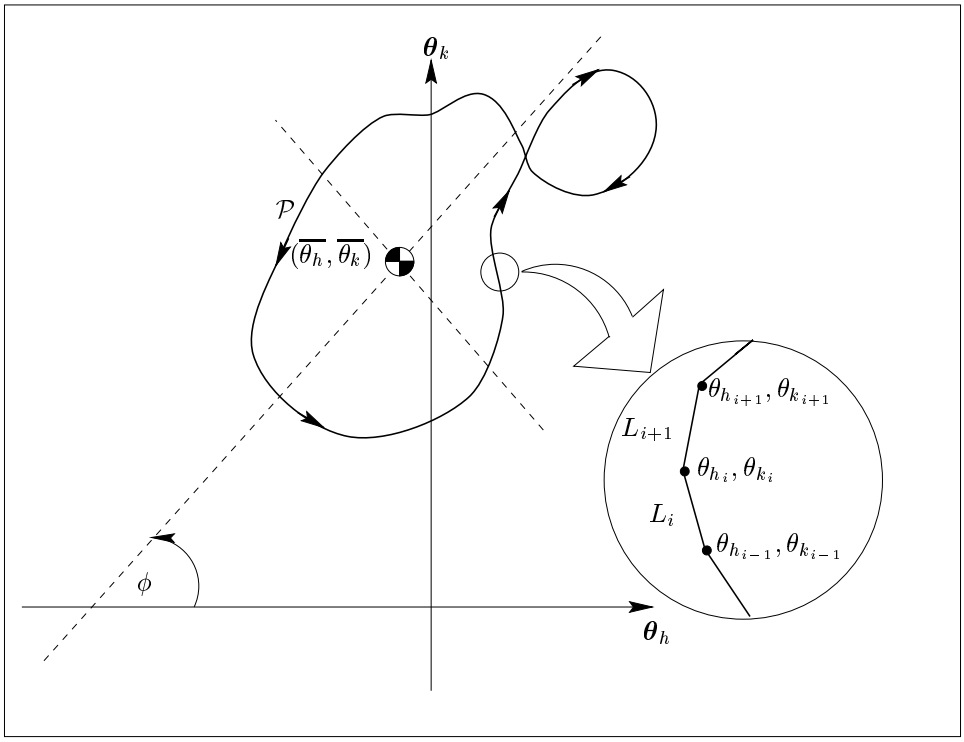

Figure 10: A plane closed curve. Certain important distinctions of the cyclograms under study are included in this sketch. Cyclograms consist of a set of unequal straight lines each line connecting two successive data points.

In order to interpret the cyclogram perimeter, we express the length of the straight line segment L_i connecting two successive data points $\theta_{h_i}, \theta_{k_i}$ and $\theta_{h_{i+1}}, \theta_{k_{i+1}}$, see Fig. 10 as,

$$\begin{aligned} L_i &= \sqrt{(\theta_{h_{i+1}} - \theta_{h_i})^2 + (\theta_{k_{i+1}} - \theta_{k_i})^2} \\ &= \Delta t_i \sqrt{(\omega_{h_i})^2 + (\omega_{k_i})^2} \end{aligned} \tag{11}$$

where ω_{h_i} and ω_{k_i} are the average angular velocities of the hip and the knee joints, respectively during the interval, and Δt_i is the corresponding time interval. Recalling that $L = \sum_{i=1}^{n} L_i$, the above equations can be extended to the entire cyclogram.

According to the first of the Eqns. 11 the cyclogram perimeter is the "total distance traveled" by the two joints in their respective joint spaces. The larger the joint excursion, the longer is the perimeter. Joint excursion is not to be confused with joint range (which we discuss later) – a joint can have a large excursion within a small range. A simple example is Fig 12 where the cyclogram on the left has a higher X-joint range but a lower X-joint excursion compared to the cyclogram on the right. Fig. 11(a) thus indicates that the total joint excursion linearly decreases as the slope changes from -13° to $+13^\circ$.

The second of Eqns. 11, on the other hand, relates the cyclogram perimeter to the average velocity of the two joints during a complete gait cycle. For cycles of equal duration, the perimeter is proportional to the average joint velocity. The duration of gait cycle is a linearly increasing function of slope as shown in Fig. 11(b). The plot of the perimeter / cycle duration ratio has the same nature as that of Fig. 11(a), only steeper. This implies that the average joint velocity linearly decreases while the slope changes from -13° to $+13^\circ$. Please note that a higher average joint velocity during a cycle does not necessarily imply a higher walking speed.

Incidentally, a longer cycle duration corresponds to a smaller value of cadence which is what we observe for uphill slopes thus precisely corroborating the observations by [53, 47].

4.2.2 Area

Although the area does not directly fall into our scheme of perimeter-based moments[7], we include it for its obvious intuitive appeal. In addition, cyclogram area is required to calculate its circularity criterion (Section 4.2.3).

The signed area of a polyline contour can be computed as

[7] In the area-based moment scheme, the area of a closed contour is its zeroth moment

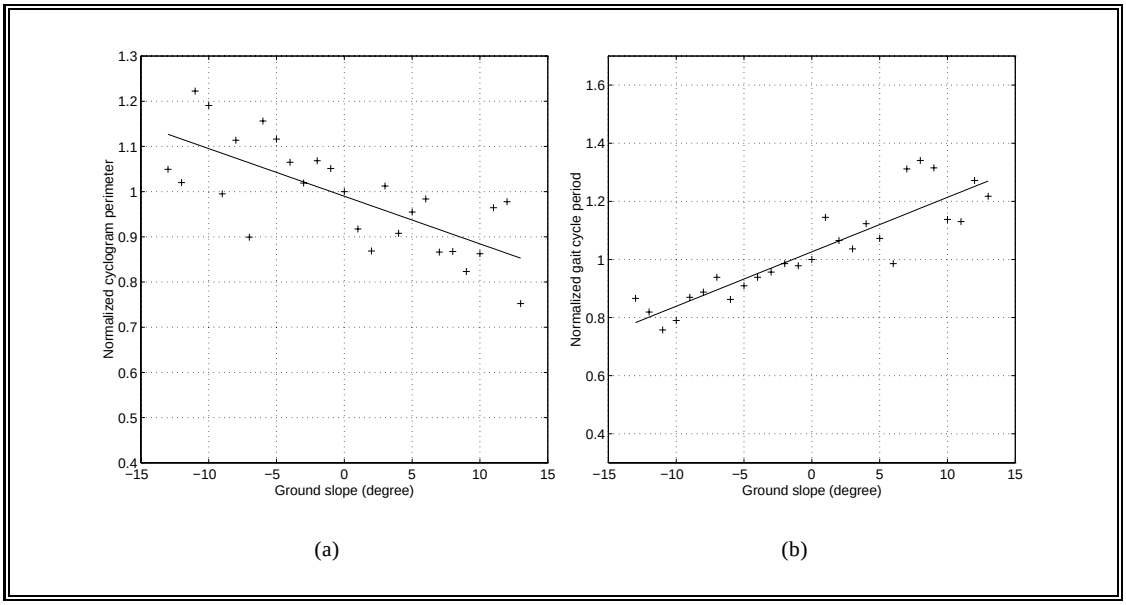

Figure 11: Evolution of normalized cyclogram perimeter and normalized gait cycle period with change in ground slope. The straight lines show linear fit of the data.

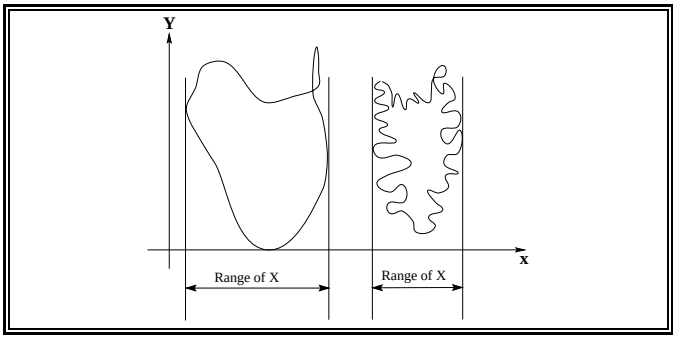

Figure 12: The difference between the joint excursion (measured by perimeter) and the joint range (related to cyclogram area) is demonstrated with artificial cyclograms. The cyclogram on the left has higher joint range but a lower joint excursion compared to that on the right.

$$A = \sum_{i=1}^{n} a_i = \sum_{i=1}^{n} x_i y_{i+1} - x_{i+1} y_i \,. \tag{12}$$

which assigns a positive value to the area inside a counterclockwise contour and a negative value to one inside a clockwise contour. This introduces errors in our calculations for cyclograms with intersecting loops.

Fig. 13(a) shows the normalized cyclogram area as a function of the ground slope. The normalization is done with respect to the area of a circle whose perimeter is equal to that of the cyclogram corresponding to the 0° slope. The parabolic line represents a quadratic fit of the data.

Noting that the cyclogram area is an indication of the conjoint range of joint movements [25] we can say that the range is maximum for level and shallow uphill slopes.

Although we are not aware of the use of cyclogram area in quantifying gait except that by [25, 24], the area inside the phase diagram, in a different context, was used to obtain a measure of gait symmetry in post-polio patients[31].

4.2.3 Circularity or compactness or roundedness

Several versions of a dimensionless criterion involving the perimeter and the area of a closed contour and characterizing its circularity, compactness or roundedness are in use in the literature. Jain[33] used the expression $\gamma = \frac{P^2}{4\pi A}$ whereas quantities such as $\frac{4\pi A}{P^2}$, $\frac{P^2}{A}$ [32], and $\frac{P}{\sqrt{A}}$ [25, 24] are also used in the literature. In this

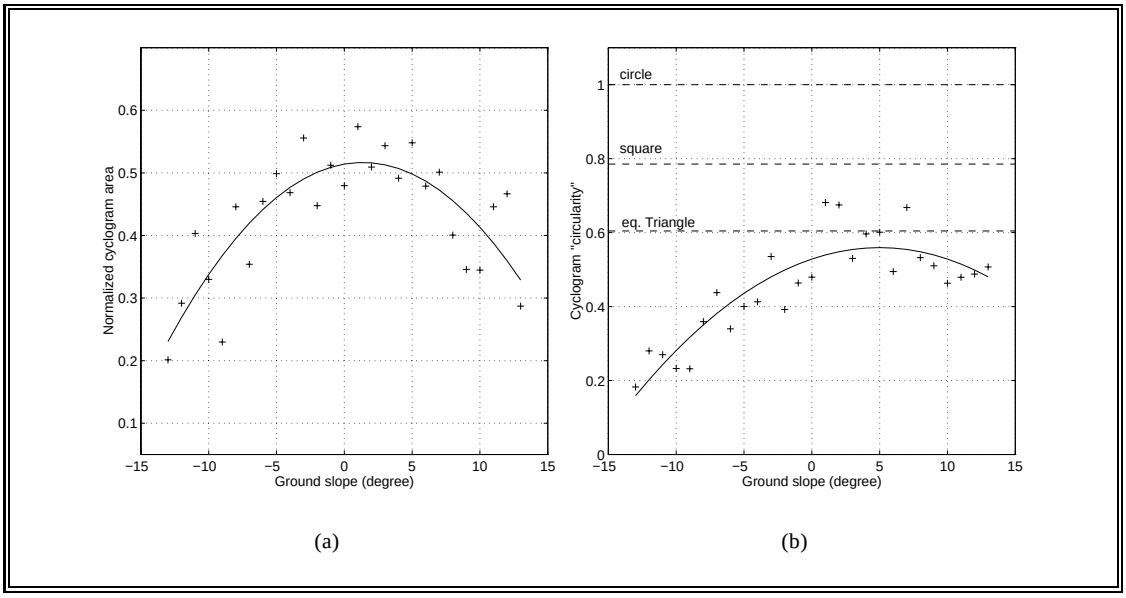

Figure 13: Evolution of normalized area and cyclogram circularity with change in ground slope. The parabolic lines represent quadratic fit of the data. In (b) the circularity of well-known geometric entities, the circle, the square and the equilateral triangle are shown for comparison.

paper, we use $\gamma = \frac{4\pi A}{P^2}$ simply because it is unity for a circle (which is the maximum possible value) and that a higher value of circularity means that the cyclogram is more circular. For comparison we note that the values of γ for a square and for an equilateral triangle are $\frac{4}{\pi}$ and $\frac{3\sqrt{3}}{\pi}$, respectively. Generally oblong objects have smaller circularity values. Fig. 13(b) presents the evolution of the circularity criterion $\frac{P^2}{A}$ as a function of the ground slope. The figure indicates that the cyclogram circularity is maximum around $+5^\circ$ slope and decreases for lower (including downhill) and higher slopes. This is qualitatively verified from Fig. 6 and 3.3. The low circularity of the negative slope cyclograms is, to a large extent, due to the fact that following the heel-strike the cyclogram trajectory reverses its direction and retraces itself thereby adding significantly to the perimeter but very little to the area.

It should however be pointed out that two significantly different shapes may possess the same circularity [56]. Also, the criterion can significantly alter between a continuous curve and its discrete counterpart, depending on the fineness of discretization.

4.2.4 Location

Location, in this context, means the position of the center of mass (CM) of a wire of uniform mass in the shape of the cyclogram. The position of the CM ($\theta_{h_{CM}}, \theta_{k_{CM}}$) is given by

$$\theta_{h_{CM}} = \frac{M_{10}}{M_{00}} \text{ and } \theta_{k_{CM}} = \frac{M_{01}}{M_{00}} \tag{13}$$

where M_{10} and M_{01} are the two first-order moments of the polygonal contour, and M_{00}, as seen before, is its perimeter.

In Fig. 14 we plot the distance of the cyclogram CM from the coordinate origin as a function of the ground slope. The distance is normalized against that of the cyclogram for 0° slope. The line of quadratic fit is also shown superposed. Fig. 14(b) shows the locus of the CM on the θ_h/θ_k plane. It is clear from the plots that the CM is the nearest to the origin for downhill walk on feeble slopes and moves away for positive as well as negative slopes.

For the joint angle assignment convention used in the paper (refer to Fig. 2) the coordinate origin of the cyclogram plane corresponds to a straight leg configuration aligned with the trunk. Thus the distance of a point from the origin to the cyclogram represents the deviation of the current configuration from this configuration. If the cyclogram CM is viewed as the "average" leg configuration during a complete walk cycle, its distance from the origin will be a quantification of the deviation of this average configuration from the passive leg configuration which is vertical[8].

[8]We note that this "average" is a purely geometric average and time is not involved in this definition.

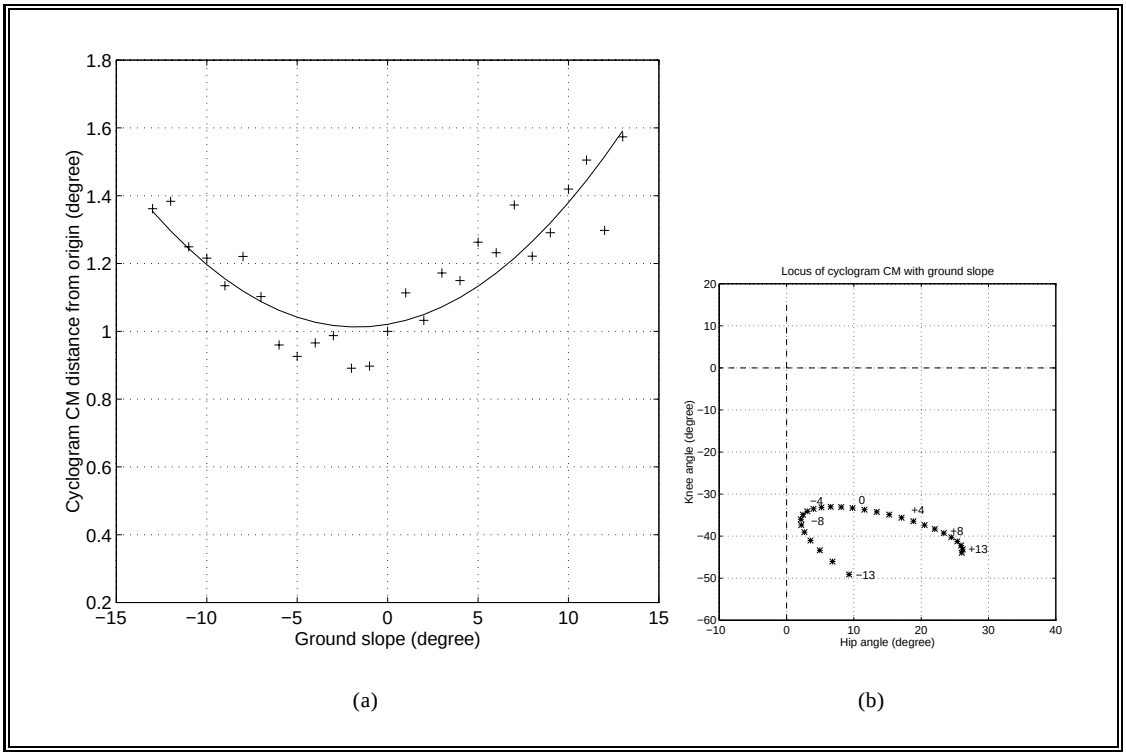

Figure 14: Evolution of cyclogram CM displacement with change in ground slope. A quadratic approximation is superposed on the data points. In the second figure we see the locus of the CM position with slope.

4.2.5 Orientation

The angle (bounded between $\pm 90^\circ$) between the positive abscissa and the line of least second-order moment of the contour is traditionally called the *orientation* of a contour. Since the line of the least second moment passes through the CM of the contour ($\theta_{h_{CM}}, \theta_{k_{CM}}$), its equation will be simpler if we displace the coordinate frames such that the new origin coincides with the center[27]. After effecting this displacement as shown in Figs. 15(a) and 15(b) the points on the curve with respect to the new origin are expressed as $\overline{\theta}_{h_i} = \theta_{h_i} - \theta_{h_{CM}}, \overline{\theta}_{k_i} = \theta_{k_i} - \theta_{k_{CM}}$. We work henceforth with points $\overline{p_i}(\overline{\theta}_{h_i}, \overline{\theta}_{k_i})$.

The moments calculated with respect to a coordinate frame situated at the CM of an object are called its *central moments* and are denoted by $\overline{M}_{pq}$. The central moments can be calculated by the same equations presented in Table 1, only the data point coordinates will have changed. In the new coordinates $\overline{M}_{10} = \overline{M}_{01} = 0$.

The orientation of the line of minimum second-order moment, ϕ is given by [32, 33]

$$\begin{aligned} sin(2\phi) &= \pm \frac{2\overline{M}_{11}}{\sqrt{4\overline{M}_{11}^2 + (\overline{M}_{20} - \overline{M}_{02})^2}} \\ cos(2\phi) &= \pm \frac{\overline{M}_{20} - \overline{M}_{02}}{\sqrt{4\overline{M}_{11}^2 + (\overline{M}_{20} - \overline{M}_{02})^2}} \end{aligned} \tag{14}$$

where $\overline{M}_{20}, \overline{M}_{11}$, and $\overline{M}_{02}$ are the three second-order central moments of the contour. The orientation of the line of maximum second-order moment is simply $\phi + 90^\circ$. In the Eqns. 14 the $+$ signs correspond to the minimum moment line whereas the $-$ signs correspond to the maximum moment line. It can be shown that the calculation of the angle ϕ is equivalent to determining the eigenvectors (the directions of the lines) and the eigenvalues (the magnitudes of the moments) of the 2×2 matrix of second moments $\begin{bmatrix} \overline{M}_{20} & \overline{M}_{11} \\ \overline{M}_{11} & \overline{M}_{02} \end{bmatrix}$.

Keeping the origin fixed at the CM, if we now rotate the coordinate frame so that it is aligned with the maximum and minimum second-order central moments, the moment calculations are much simplified. Fig. 15(c) shows this coordinate frame alignment procedure. In the rotated coordinate frame $\overline{M}_{11} = 0$ and the moment matrix written above is diagonal.

The most characteristic feature in the evolution of orientation with ground slope (Fig. 16) is the two constant orientation regions connected by a discrete jump which occurs around $+5^\circ$ slope. Visual inspection

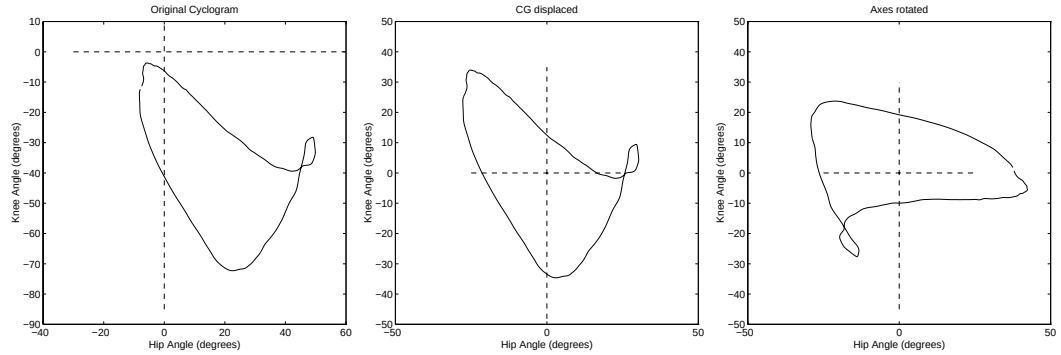

(a) Cyclogram (b) Origin shifted to CM. (c) Axes aligned with principal 2^{nd}-order moments.

Figure 15: The displacement and rotation of the coordinate frames to simplify moment calculations.

of Fig. 3.3 convinces us that the cyclograms for higher uphill slopes are decidedly inclined. The orientation analysis quantifies this geometric feature.

4.2.6 Eccentricity and the best fit ellipse

There are several definitions of eccentricity of a closed planar contour the simplest of which is the ratio of the maximum and minimum second moments[27]. Eccentricity is also an indication of the oblongness of the contour, and is thus related to the circularity criterion. We however prefer using eccentricity which is conveniently based on perimeter-based moments and no calculation of area is needed. Fig. 16(b) represents the evolution of cyclogram eccentricity with respect to ground slope. A cubic polynomial approximation of the data is shown superposed.

The above definition of eccentricity is ill-conditioned for extremely elongated shapes. According to this definition the eccentricity of a circle is unity but that of a line is infinity (as the minimum second moment for a line is zero). A better definition is thus [32]

$$\varepsilon = \frac{(\overline{M}_{20} - \overline{M}_{02})^2 + 4\overline{M}_{11}^2}{(\overline{M}_{20} + \overline{M}_{02})^2}, \tag{15}$$

according to which the curve of minimum eccentricity is a circle which has $\varepsilon = 0$ and for a straight line $\varepsilon = 1$.

In yet another approach the eccentricity of a contour is defined as the ratio of the lengths of the semi-major and the semi-minor axes of the best-fit ellipse of the contour. The best-fit ellipse is the ellipse which has the same second-order moment matrix as that of the contour. Let a and b be the semi-major and the semi-minor axes, respectively, of the best-fit ellipse. The least and the greatest moments of inertia of the ellipse are

$$m_{2_{min}} = \frac{\pi}{4}ab^3, \text{ and } m_{2_{max}} = \frac{\pi}{4}a^3b \tag{16}$$

For the best-fit ellipse we have[33]

$$a = (\frac{4}{\pi})^{\frac{1}{4}}[\frac{(m_{2_{max}})^3}{m_{2_{min}}}]^{\frac{1}{8}}, \text{ and } b = (\frac{4}{\pi})^{\frac{1}{4}}[\frac{(m_{2_{min}})^3}{m_{2_{max}}}]^{\frac{1}{8}} \tag{17}$$

The nature of the plots of the two latter definitions of eccentricity are very similar to that of the former.

4.2.7 Quantification of cyclogram evolution

In order to demonstrate how we can provide a global picture of the evolution of cyclograms with the help of the gait descriptors we plot in a 3D space two different triplets. In the first figure (Fig. 17) the normalized perimeter, the ratio of maximum and minimum second moments and the distance of the cyclogram CM from the origin for each slope are plotted. We have used data from the line fits for this plot shown in Fig. 17. In the second plot we have shown the normalized cyclogram area, circularity and the normalized cycle duration.

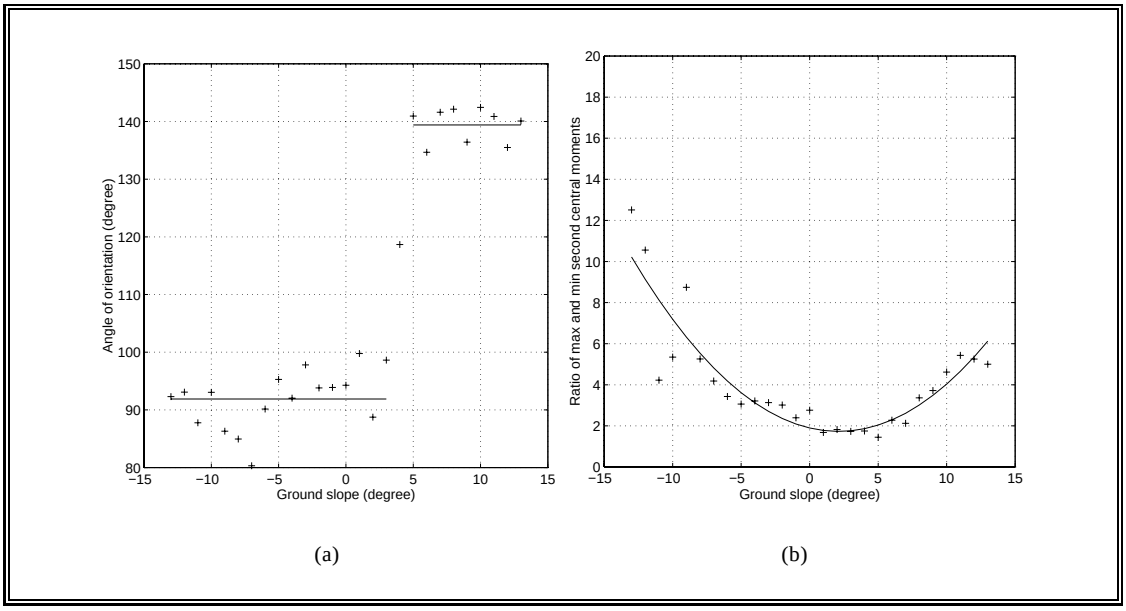

Figure 16: Evolution of a) cyclogram orientation and b) the ratio of maximum and minimum second central moments with change in ground slope. The first curve is fitted with two constants. The line in the second figure shows cubic fit of the data.

These figures represent signatures of normal walking of the subject by compactly capturing a multitude of information.

4.2.8 Higher order moments – an invariant of slope walking?

The higher order central moments of the contour are calculated with respect to the coordinate axes fixed to the CM and aligned with the maximum and minimum second moments. The alignment is done by means of multiplying each data point by means of a rotation matrix $\boldsymbol{R}$ as

$$\boldsymbol{p}' = \boldsymbol{R}\boldsymbol{p} \tag{18}$$

where $\boldsymbol{R} = \begin{bmatrix} cos\phi & -sin\phi \\ sin\phi & cos\phi \end{bmatrix}$ and ϕ is the orientation angle of the contour.

In general, unless normalized, the higher order moments have high numerical values as we can anticipate from Eq. 1. Moreover they are known to be sensitive to noise which means a small change in the cyclogram will cause a large change in the moments. The evolutions of the four third-order cyclogram moments are shown in the top row of Fig. 18. There is no apparent regularity in the these curves. However if we consider the ratios of $\frac{\overline{M}_{03}}{\overline{M}_{30}}$ and $\frac{\overline{M}_{12}}{\overline{M}_{21}}$ as shown in the bottom line of Fig. 18 we notice that in a remarkable manner these quantities stay constant for the entire range of positive and negative slopes. The plot of $\frac{\overline{M}_{03}}{\overline{M}_{30}}$ is shown with two constant data fits as there is a discrete (but not of large magnitude) jump in the plot around 5° uphill slope. In the plot of $\frac{\overline{M}_{12}}{\overline{M}_{21}}$ we have suppressed the value (=-21.537) corresponding to $+6^\circ$ slope which we considered to be an outlier. It is rather interesting to note that in spite of the large magnitudes of these moments (orders of 10^4 to 10^5) their ratios stay remarkably constant. Even without a concrete physical interpretation of the third-order cyclogram moments, these quantities have the potential to play the role of *invariants* of slope-walking.

Another candidate for invariant is obtained from what are called the *moment invariants*. These are the combinations of moments of a certain order which are insensitive to rotation and reflection of the contour considered. Two third-order invariants [33] are $\sigma_1 = (\overline{M}_{30} + \overline{M}_{12})^2 + (\overline{M}_{03} + \overline{M}_{21})^2$ and $\sigma_2 = (\overline{M}_{30} - 3\overline{M}_{12})^2 + (\overline{M}_{03} - 3\overline{M}_{21})^2$. The ratio $\frac{\sigma_2}{\sigma_1}$, turns out to be a good candidate of invariant in slope-walking as confirmed from Fig. 19. Again, in this case the high value of the ratio for -13° slope is perhaps an outlier.

5 Discussion

Gait parameterization by means of cyclogram moments can be of potential use in a number of fields such as the quantitative characterization of normal gait, global comparison of two different gaits, clinical identification of pathological conditions and in the tracking of the progress of patients under rehabilitation program.

What has been achieved up till now is the establishment of a standard cyclogram corresponding to the normal walk and the recognition of the fact that the cyclograms continuously deform in a predictable manner as the ground slope changes. Exploiting the concept of perimeter-based moments, each cyclogram has been assigned with a set of numbers that quantify its geometric characteristics. The standard qualitative features of the hip-knee cyclograms for uphill and downhill walk are acknowledged in the literature. Based on this we can expect that the general trends of the slope walking gait descriptors will be similar for all individuals. What is to be seen is whether the precise moment-values reported in this work are also subject-independent.

In order for the cyclograms to become an effective tool for the clinical identification of pathological conditions we need the analytical skill of correlating a pathology with a corresponding feature of the cyclogram. This necessitates a thorough acquaintance with all the pertinent cyclogram patterns available from the human gait. However, if we represent a cyclogram as a point in a multidimensional space capturing all its moments, a pathology might be suspected or identified by noting the position of this point relative to other points representing normal gaits. One can imagine judiciously adding other axes in the multidimensional space in order to make this procedure more robust. Thus more work in concert with the clinicians is necessary.

As a patient under rehabilitation care returns to a normally functioning gait so should his gait cyclograms. A scalar quantification of the difference between the patient's gait from a normal gait is the multidimensional distance between the points (similar to those mentioned in the above paragraph) representing the two gaits. The locus of this point over several weeks is a signature of the process of rehabilitation.

Improvements of the presented technique should include a proper treatment of the multiple and self-included loops, as these are often encountered. A second necessity is that of a comprehensive sensitivity analysis. The sensitivity of the cyclogram moments with respect to different data smoothing / filtering algorithms might indicate the appropriateness of different algorithms. It seems more reasonable to perform statistical analyses on the gait descriptors obtained from different gait cycles than to perform averaging of the data before extracting a standard set of gait descriptors from the averaged data. More work needs to be done to verify this.

Gait analysis performed on the basis of the entire cycle rather than from discrete measures such as step length has some advantages as mentioned earlier. It is quite likely that a meaningful normalization of the cyclograms would significantly improve the results. One can imagine normalizations based on cycle duration, leg length or body mass. Another approach is to treat the cyclogram as a purely geometric form. Such a normalization – for example, constraining the entire cyclogram to lie inside a unit square – would complicate the physical interpretation. We underline the fact that the algorithms for moment calculations are directly applicable to other closed curves and thus gait parameterization could be performed as well with moment-angle diagrams[18], phase diagrams[4, 31, 30] or velocity-velocity curves[51]. It is also possible to use other shape parameters such as the bending energy of the cyclogram perimeter [56] or its electric potential[11] as gait descriptors.

Acknowledgments

Helpful discussions with Bernard Espiau, Research Director of INRIA Rhône-Alpes are gratefully acknowledged. Emmanuel Cordier, a Ph.D. candidate at INRIA Rhône-Alpes coordinated the experiments described in this work. Prof. Jean-Pierre Blanchi of the laboratory UFR STAPS at Joseph Fourier University, Grenoble lent us his data registration system and Prof. Alain Belli of Laboratory of Exercise Physiology, GIP Exercise, St. Etienne made his laboratory equipped with a variable inclination treadmill available to us. A preliminary version of the slope-walking experiment was performed on a fixed 10° slope in the UFR STAPS Movement Analysis Group laboratory of Prof. Thierry Pozzo in the University of Dijon. Their help is sincerely acknowledged.

References

[1] R R. Bailey and M Srinath. Orthogonal moment features for use with parametric and non-parametric classifiers. *IEEE Transactions Pattern Analysis and Machine Intelligence*, 18(4):389–399, 1996.

[2] J. G. Barton and A. Lees. An application of neural networks for distinguishing gait patterns on the basis of hip-knee joint angle diagrams. *Gait & Posture*, 5:28–33, 1997.

[3] P. Bergé, Y. Pomeau, and C. Vidal. *Order within chaos*. John Wiley & sons, New York, 1984.

[4] A. Beuter and A. Garfinkel. Phase plane analysis of limb trajectories in non-handicapped and cerebral palsied subjects. *Adapted Physical Activity Quarterly*, 2:214–227, 1985.

[5] A. C. Bobbert. Energy expenditure in level and grade walking. *Journal of Applied Physiology*, 15:1015–1021, 1960.

[6] N. A. Borghese, L. Bianchi, and F. Lacquaniti. Kinematic determinants of human locomotion. *Journal of Physiology*, 494(3):863–879, 1996.

[7] P. Cavanagh. *Biomechanics of Distance Running*. Human Kinetics Books, Champaign, IL, 1990.

[8] P. Cavanagh and D. W. Grieve. The graphical display of angular movement of the body. *British Journal of Sports Medicine*, 7:129–133, 1973.

[9] J. Charteris. Human gait cyclograms: Conventions, speed relationships and clinical applications. *International Journal of Rehabilitation Research*, 5(4):507–518, 1982.

[10] J. Charteris, D. Leach, and C. Taves. Comparative kinematic analysis of bipedal and quadrupedal locomotion: A cyclographic technique. *Journal of Anatomy*, 128(4):803–819, 1979.

[11] J-H. Chuang. A potential-based approach for shape matching and recognition. *Pattern Recognition*, 29(3):463–470, 1996.

[12] E. Cordier. Automatic method for cycle extraction and segmentation in human gait kinematic data. In *XVIth Congress of the International Society of Biomechanics, Tokyo*, August 1997.

[13] E. Cordier, A. Goswami, and M. Bourlier. Kinematic parameterization of natural slope walking. In *13th Symposium Posture and Gait, Paris*, June 1997.

[14] L. Erickson, E. Simonson, H. L. Taylor, H. Alexander, and A. Keys. The energy cost of horizontal and grade walking on the motor-driven treadmill. *American Journal of Physiology*, (145):391–401, 1946.

[15] B. Espiau. Bip: A joint project for the development of an anthropomorphic biped robot. In *Proc. of the International Conference on Advanced Robotics*, July 1997.

[16] F.R. Finley and K. A. Cody. Locomotive characteristics of urban pedestrians. *Archives of Physical Medicine and Rehabilitation*, 51:423–426, 1970.

[17] H. Freeman. Computer processing of line-drawing images. *Computing Surveys*, 6(1):57–97, 1974.

[18] C. Frigo, P. Crema, and L. M. Jensen. Moment-angle relationship at lower limb joints during human walking at different velocities. *Journal of Electromyography and Kinesiology*, 6(3):177–190, 1996.

[19] R.C. Gonzalez and P. Wintz. *Digital Image Processing*. Addison-Wesley Publishing Company, Reading, MA, 1987.

[20] A. Goswami and E. Cordier. Moment-based parameterization of cyclograms of slope-walking. In *XVIth Congress of the International Society of Biomechanics, Tokyo*, August 1997.

[21] A. Goswami, B. Thuilot, and B. Espiau. Compass-like biped robot part i: Stability and bifurcation of passive gaits. Technical report, INRIA, No. 2996, Oct. 1996.

[22] D.W. Grieve. Gait patterns and the speed of walking. *Biomedical Engineering*, 3:119–122, 1968.

[23] D.W. Grieve. The assessment of gait. *Physiotherapy*, 55:452–460, 1969.

[24] C. Hershler and M. Milner. Angle-angle diagrams in above-knee amputee and cerebral palsy gait. *American Journal of Physical Medicine*, 59(4):165–183, 1980.

[25] C. Hershler and M. Milner. Angle-angle diagrams in the assessment of locomotion. *American Journal of Physical Medicine*, 59(3):109–125, 1980.

[26] R. C. Hilborn. *Chaos & Nonlinear Dynamics*. Oxford University Press Inc., Oxford, UK, 1994.

[27] B.K.P. Horn. *Robot Vision*. The MIT Press, Cambridge, MA, 1986.

[28] M-K. Hu. Visual pattern recognition by moments invariants. *IRE Transactions on Information Theory*, IT-8(8):179–187, 1962.

[29] Y. Hurmuzlu and C. Basdogan. On the measurement of stability in human locomotion. *ASME Journal of Biomechanical Engineering*, 116:30–36, 1994.

[30] Y. Hurmuzlu, C. Basdogan, and J. J. Carollo. Presenting joint kinematics of human locomotion using phase plane portraits and poincaré maps. *Journal of Biomechanics*, 27(12):1495–1499, 1994.

[31] Y. Hurmuzlu, C. Basdogan, and D. Stoianovici. Kinematics and dynamic stability of locomotion of polio patients. *ASME Journal of Biomechanical Engineering*, 118:405–411, 1996.

[32] B. Jahne. *Digital Image Processing*. Springer-Verlag, Berlin, 1995.

[33] A.K. Jain. *Fundamentals of Digital Image Processing*. Prentice-Hall International, Inc., Englewood Cliffs, N.J., 1989.

[34] X.Y. Jiang and H. Bunke. Simple and fast computation of moments. *Pattern Recognition*, 24(8):801–806, 1991.

[35] K. Kawamura, A. Tokuhiro, and H. Takechi. Gait analysis of slope walking: a study on step length, stride width, time factors, and deviation in the center of pressure. *Acta Medica Okayama*, 45(3):179–184, 1991.

[36] B. Kuo. *Automatic Control*. Prentice-Hall International, Inc., Englewood Cliffs, N.J., 1990.

[37] L. W. Lamoreux. Kinematic measurements in the study of human walking. *Bulletin of Prosthetics Research*, BPR 10-15 (spring):3–84, 1971.

[38] B-C. Li and J. Shen. Fast computation of moments invariants. *Pattern Recognition*, 24(8):807–813, 1991.

[39] S.X. Liao and M. Pawlak. On image analysis by moments. *IEEE Transactions Pattern Analysis and Machine Intelligence*, 18(3):254–266, 1996.

[40] M. Milner, D. Dall, V. A. McConnel, P. K. Brennan, and C. Hershler. Angle diagrams in the assessment of locomotor function. *S.A. Medical Journal*, 47:951–957, 1973.

[41] K. M. Newell. Coordination, control and skill. In D. Goodman, R.B. Wilverg, and I. M. Franks, editors, *Differing Perspectives in Motor Learning, Memory and Control*, pages 295–317. Amsterdam: North-Holland, 1985.

[42] M. S. Redfern and J. J. DiPasquale. Biomechanics of descending ramps in young and elderly. In *Fifth Injury Prevention Through Biomechanics Symposium*, 1995.

[43] J. Serra. *Image analysis and mathematical morphology : 1*. Academic press, Paris, 1982.

[44] D. C. Shapiro, R. F. Zernicke, R. J. Gregor, and J. D. Diestel. Evidence of generalized motor programs using gait pattern analysis. *Journal of Motor Behavior*, 13(1):33–47, 1981.

[45] K.J. Simpson, P. Jiang, P. Shewokis, S. Odum, and K. Reeves. Kinematic and plantar pressure adjustments to downhill gradients during gait. *Gait & Posture*, 1:172–179, 1993.

[46] J.W. Snellen. External work in level and grade walking on a motor-driven treadmill. *Journal of Applied Physiology*, 15:759–763, 1960.

[47] J. Sun, M. Walters, N. Svensson, and D. Lloyd. The influence of surface slope on human gait characteristics: a study of urban pedestrians walking on an inclined plane. *Ergonomics*, 39(4):677–692, 1996.

[48] M.R. Teague. Image analysis via the general theory of moments. *J. of Optical Soc. of America*, 70(8):920–930, 1980.

[49] J.C. Wall and J. Charteris. The temporal and angular kinematics of uphill and downhill walking. *unpublished*, 1993.

[50] J.C. Wall, J.W. Nottrodt, and J. Charteris. The effects of uphill and downhill walking on pelvic oscillations in the transverse plane. *Ergonomics*, 24(5):807–816, 1981.

[51] W. C. Whiting and R. F. Zernicke. Correlation of movement patterns via pattern recognition. *Journal of Motor Behavior*, 14(2):135–142, 1982.

[52] M. Yamasaki and T. Sasaki. Autoregressive analysis of step length in level and grade walking. *Kumamoto Medical Journal*, 41:51–62, 1989.

[53] M. Yamasaki, T. Sasaki, S. Tsuzuki, and M. Torii. Stereotyped pattern of lower limb movement during level and grade walking on treadmill. *Annals of Physiological Anthropology*, 3(4):291–296, 1984.

[54] L. Yang and F. Albregtsen. Fast and exact computation of cartesian geometric moments using discrete green's theorem. *Pattern Recognition*, 29(7):1061–1074, 1996.

[55] T. Yokoi, A. Takahashi, and K. O. Byun. Self-organization of lower limb motion in human locomotion. *Journal of Robotics and Mechatronics*, 8(4):364–371, 1996.

[56] I. T. Young, J. E. Walker, and J. E. Bowie. An analysis technique for biological shape. *Information and Control*, 25:357–370, 1974.

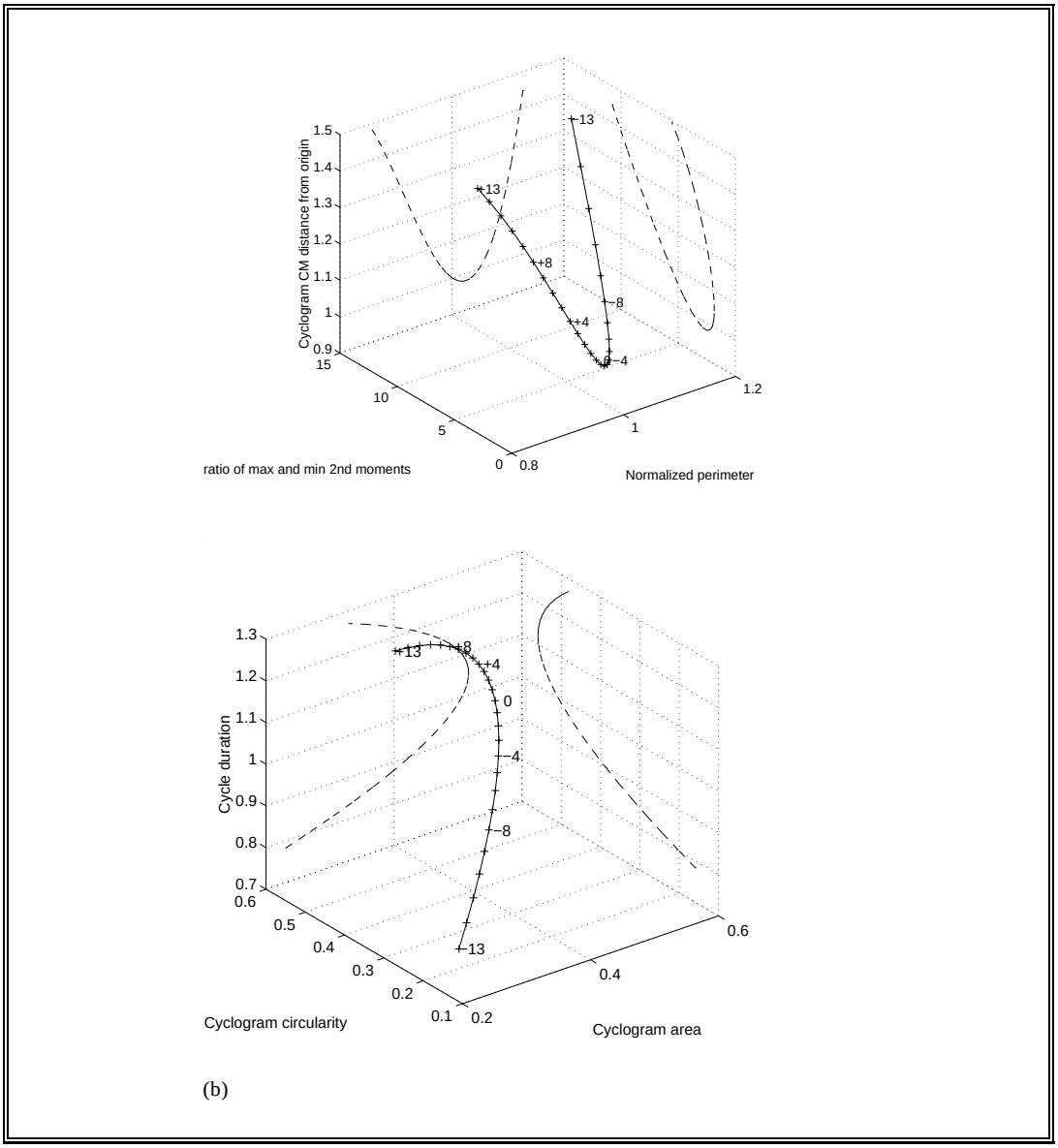

Figure 17: The evolution of a) normalized perimeter, the ratio of maximum and minimum second moments and the distance of the cyclogram CM from the origin and b) normalized cyclogram area, circularity and the normalized cycle duration, with respect to ground slope. The projection of the curve on the two vertical planes are shown in dashed lines.

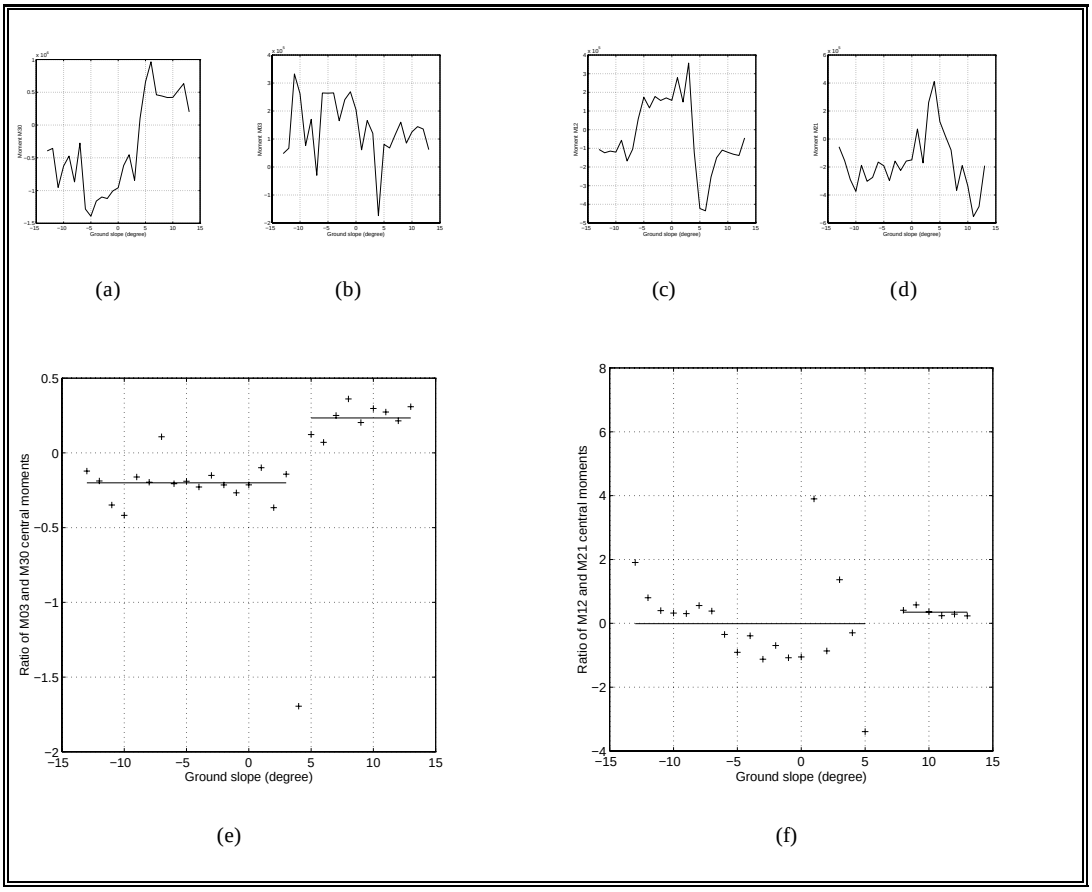

Figure 18: Evolution of the ratio of e) $\overline{M_{03}}$ and $\overline{M_{30}}$ and f) $\overline{M_{12}}$ and $\overline{M_{21}}$ with change in ground slope. The four smaller curves a, b, c and d show the evolution of the individual second-order moments $\overline{M_{30}}$, $\overline{M_{03}}$, $\overline{M_{12}}$ and $\overline{M_{21}}$.

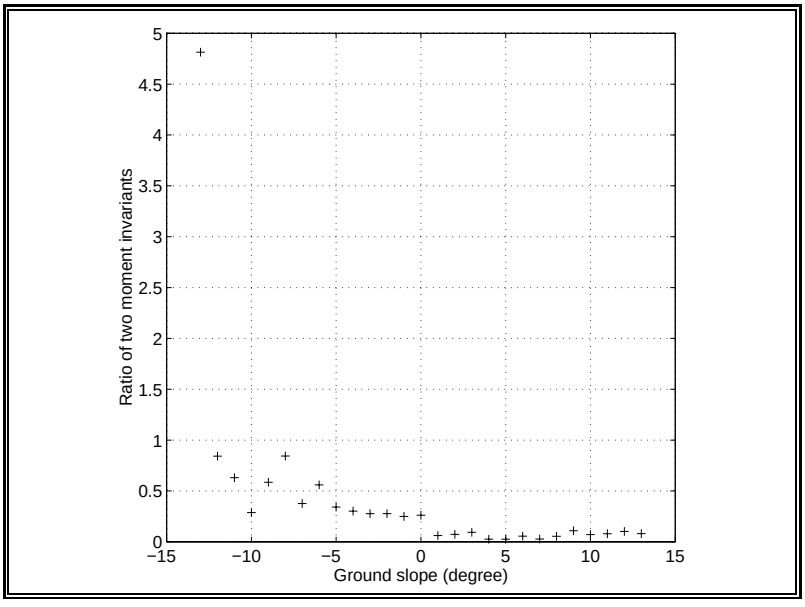

Figure 19: Evolution of the ratio of two third-order moment invariants with change in ground slope.